

**RESPONSE OF AIRCRAFT TO THREE
DIMENSIONAL RANDOM TURBULENCE**


*FREDERICK D. EICHENBAUM
LOCKHEED-GEORGIA COMPANY*

FOREWORD

This report was prepared by Lockheed-Georgia Company, Marietta, Georgia, under Air Force Contract F33615-71-C-1878. The contract was initiated under Project Number 1367, "Structural Design Criteria", Task Number 136702. The work was administered under the direction of the Air Force Flight Dynamics Laboratory, Research and Technology Division, Air Force Systems Command, Wright-Patterson Air Force Base, Ohio, Mr. Paul L. Hasty (FBE-B), Project Engineer.

The work reported in this study was conducted by Lockheed-Georgia Company with Frederick D. Eichenbaum as principal investigator, and covers the period July 1971 to March 1972. The report was submitted by the author in March 1972.

This technical report has been reviewed and is approved.


Gordon R. Negaard, Major, USAF
Chief, Design Criteria Branch
Structures Division

ABSTRACT

Conceptually possible procedures for designing aircraft for the combined effects of vertical, lateral, and longitudinal turbulence by the application of power spectral techniques are developed and outlined. The present state-of-the-art of this technical area is established and evaluated by reviewing and extending current methods used or proposed for predicting the response of aircraft due to combined effects of the three components of atmospheric turbulence. Requirements for solving the problem are identified and recommendations are made with respect to major problem areas such as: description of the turbulence environment, determination of the frequency response function of the structure, and methods of combining the effects of vertical, lateral and longitudinal turbulence components to theoretically predict aircraft response. Finally, an outline of the specific research needed is given, and a program is presented for accomplishing the research and development required to solve the problem.

Contrails

TABLE OF CONTENTS

<u>Section</u>	<u>Title</u>	<u>Page</u>
I	INTRODUCTION	1
II	TECHNICAL BACKGROUND	4
	2.1 Frequency Response Functions	4
	2.2 Three-Dimensional Turbulence	5
	2.3 Nonredundant Space Domain Formulation	13
	2.4 Panel Summation Form	18
	2.5 Gust Velocity Coherence Tensor	20
	2.6 Transfer Functions	21
	2.7 Coupling between Gust Components	23
	2.8 Cross Transfer Functions	24
III	AIRCRAFT DESCRIPTION	27
	3.1 Governing Equation	27
	3.2 Modal Analysis	28
	3.3 Detailed Solution	29
	3.4 Loads and Deflections	31
	3.5 Frequency Response Functions	32
	3.6 Symmetry Considerations	33
IV	THREE-DIMENSIONAL GUST RESPONSE	34
	4.1 Response Cross Spectra	34
	4.2 Modal Cross Spectra	35
	4.3 Nondimensional Coherence Tensor	36
	4.4 Computational Procedures	51

TABLE OF CONTENTS (Continued)

<u>Section</u>	<u>Title</u>	<u>Page</u>
	4.5 One-Dimensional Turbulence Limit	53
	4.6 Improvements in Aircraft Design and Analysis	55
V	OUTLINE OF RECOMMENDED RESEARCH	59
	5.1 Implementation of Computational Methods	60
	5.2 Validation by Flight Test Comparison	62
	5.3 Applications to Aircraft Design Procedures	66
	5.4 Advanced Development	67
	REFERENCES	69
Appendix A	A DUAL GUST RESPONSE FORMULATION	72
	A.1 Space Domain	72
	A.2 Wave Domain	75
Appendix B	AN IMPROVED KERNEL FUNCTION FORMULATION FOR UNSTEADY SUBSONIC FLOW	77

LIST OF ILLUSTRATIONS

<u>Figure</u>	<u>Title</u>	<u>Page</u>
1	Unit Directional Vector Pairs Corresponding to Symmetric (+) and Antisymmetric (-) Normalwash Input Configurations	6
2	Resolution of Gust Velocity into Symmetric (+) and Antisymmetric (-) Subfields	8
3	Decomposition of a Three-Dimensional Turbulence Velocity Field	9
4	Decomposition of a Two-Dimensional Turbulence Velocity Field	11
5	Decomposition of a One-Dimensional Turbulence Velocity Field	12
6	Representation of the Gust Velocity Cross Spectrum Tensor in the Rotated Coordinate System	15
7	Normalwash Input Configurations for Calculating Symmetric and Antisymmetric Normalwash Cross Spectra	19
8	Power Spectra of Longitudinal and Transverse Gust Velocity Components Plotted vs. Reduced Frequency for the Dryden Case	40
9	Coherence between Longitudinal Gust Components Plotted vs. Lateral Separation and Reduced Frequency for the Dryden Case	41

LIST OF ILLUSTRATIONS (Continued)

<u>Figure</u>	<u>Title</u>	<u>Page</u>
10	Imaginary Part of Coherence between Longitudinal and Lateral Gust Components Plotted vs. Lateral Separation and Reduced Frequency for the Dryden Case	42
11	Excess of Coherence between Lateral Gust Components over Vertical Plotted vs. Lateral Separation and Reduced Frequency for the Dryden Case	43
12	Coherence between Vertical Gust Components Plotted vs. Lateral Separation and Reduced Frequency for the Dryden Case	44
13	Power Spectra of Longitudinal and Transverse Gust Velocity Components Plotted vs. Reduced Frequency for the von Karman Case	45
14	Coherence between Longitudinal Gust Components Plotted vs. Lateral Separation and Reduced Frequency for the von Karman Case	46
15	Imaginary Part of Coherence between Longitudinal and Lateral Gust Components Plotted vs. Lateral Separation and Reduced Frequency for the von Karman Case	47
16	Excess of Coherence between Lateral Gust Components over Vertical Plotted vs. Lateral Separation and Reduced Frequency for the von Karman Case	48

LIST OF ILLUSTRATIONS (Continued)

<u>Figure</u>	<u>Title</u>	<u>Page</u>
17	Coherence between Vertical Gust Components Plotted vs. Lateral Separation and Reduced Frequency for the von Karman Case	49
18	Proposed System for Substantiating Three-Dimensional Gust Response Analysis Methods	63
19	Behavior of the Integrals, $I_\nu(k_1, u_1)$, Occurring in the Conventional Version of the Nonplanar Acceleration Potential Kernel for Oscillating Subsonic Flow	79
20	Behavior of the Integrals, $\bar{F}_\nu(k_1, u_1)$, Occurring in the New Formulation of the Nonplanar Acceleration Potential Kernel for Oscillating Subsonic Flow	82

NOMENCLATURE

Scalars, Vectors and Dyadics:

B	Coefficient used in analytical form of $\psi_{ij}(\eta, \kappa)$
C(τ)	= $\langle X(t)X(t+\tau) \rangle$ = Autocorrelation function of a dynamic response
f	Frequency
F_v, \bar{F}_v, \tilde{F}_v	Modified, normalized and asymptotic versions, respectively, of integral I _v
G_v	Frequency-independent part of K' _v
h(r, τ)	Vector impulse response function whose components are the impulse response functions with respect to the corresponding components of the normalwash at point r
H(r, f)	= $\int \mathbf{h}(\mathbf{r}, \tau) e^{-2\pi i f \tau} d\tau$ = Vector frequency response function in the space domain whose components are the frequency response functions with respect to the corresponding components of the normalwash at point r
H(f)_{ijk}	Moment ijk of the vector frequency response function in the space domain
H (r , f)	Frequency response function with respect to normalwash at point r
H_n (f)	Frequency response function with respect to normalwash at panel n

NOMENCLATURE (Continued)

Scalars, Vectors and Dyadics:

$H_{ij}(f)$	Cross transfer function between gust velocity component i at the probe and response to gust component j
$H_i(f)$	Cross transfer function with respect to gust velocity component i measured at the probe for three-dimensional turbulence
$H_i(f)$	Cross transfer function with respect to gust velocity component i for one-dimensional turbulence
i	$\sqrt{-1}$
$\mathbf{i}, \mathbf{j}, \mathbf{k}$	Coordinate vectors of the aircraft system
$\bar{\mathbf{i}}, \bar{\mathbf{j}}, \bar{\mathbf{k}}$	Coordinate vectors of the rotated aircraft system
$I_\nu(u_1, k_1)$	Integral appearing in K
k_1	Reduced frequency variable in K
K	Doublet lattice kernel function
K_n	Modified Bessel function of the second kind of order n
K_ν	Component of doublet lattice kernel function ($\nu = 1, 2$)
K'_ν	Modified version of K_ν
$\mathbf{K}(\boldsymbol{\Omega}, f)$	$= \int \mathbf{H}(\mathbf{r}, f) e^{i\boldsymbol{\Omega} \cdot \mathbf{r}} d\mathbf{r} =$ Vector frequency response function in the wave domain
L	Scale of turbulence

NOMENCLATURE (Continued)

Scalars, Vectors and Dyadics:

M	Mach number
$\mathbf{n}(\mathbf{r})$	Unit vector in normalwash direction at aerodynamic surface point \mathbf{r}
N_0	Zero crossing rate
p	Amplitude of oscillating pressure dipole used in doublet lattice formulation
\mathbf{p}	Gust probe position vector
q	Transverse separation distance; dynamic pressure in formulation of K
\mathbf{q}	Position or separation vector; transverse separation vector
$\mathbf{Q}(\mathbf{r}, \tau)$	$= \langle \mathbf{u}(\mathbf{s}, t) \mathbf{u}(\mathbf{s} + \mathbf{r}, t + \tau) \rangle = \mathbf{R}(\mathbf{r} + \mathbf{U}\tau, \tau)$ = Correlation tensor between the gust velocities separated by (\mathbf{r}, τ) in the aircraft system
r_1, R	Transverse distance and total distance, respectively, between sending and receiving points in formulation of K
$\mathbf{R}(\mathbf{r}, \tau)$	Correlation tensor between gust velocities separated by (\mathbf{r}, τ) in the fixed reference frame
\mathbf{r}, \mathbf{s}	position or separation vectors

NOMENCLATURE (Continued)

Scalars, Vectors and Dyadics:

$\mathbf{S}(\Omega)$	$= (1/2\pi)^3 \int \mathbf{R}(\mathbf{r}, 0) e^{-i\Omega \cdot \mathbf{r}} d\mathbf{r} =$ Gust velocity power spectrum tensor in the wave domain
$\mathbf{S}(f)_{mn}$	Moment mn of the gust velocity power spectrum tensor in the wave domain
t	Time
T_ν	Geometrical parameter appearing in formulation of K ($\nu = 1, 2$)
$T_{ij}^2(f)$	Squared transfer function with respect to gust velocity components i and j for three-dimensional turbulence
$T_i(f)$	$= [\phi(f)/\Phi_i(f)]^{1/2} =$ Flight-measured transfer function with respect to gust velocity component i
u_1	Variable in K
$\mathbf{u}(\mathbf{r}, t)$	Incremental gust velocity in the aircraft system
\mathbf{U}	$= (-U, 0, 0) =$ Velocity of the aircraft in the fixed reference frame
x, y, z	Cartesian coordinates
x_0, y_0, z_0	Relative coordinates between sending and receiving points in formulation of K
$X(t)$	Dynamic response amplitude

NOMENCLATURE (Continued)

Scalars, Vectors and Dyadics:

α	Time lag
β	Time lag
γ_r	Dihedral angle at point r
$\gamma_1^2(f)$	Coherence function between the response and gust velocity component i measured at the probe
Γ	Gamma function
$\Gamma(r, f)$	Coherence tensor between gust velocities separated by r in the aircraft system
δ	Computational parameter used in formulation of K'
η	Nondimensional transverse separation distance
θ	Computational parameter used in formulation of K'
$\theta_{ij}(r, s, f)$	Coherence between normalwash components i and j at aerodynamic surface points r and s , respectively
$\theta_{ijmn}(f)$	Coherence between normalwash components i and j at aerodynamic panels m and n , respectively
κ	Nondimensional reduced frequency
λ	Gust wavelength

NOMENCLATURE (Continued)

Scalars, Vectors and Dyadics:

$\Lambda_{ij}(\mathbf{p}, \mathbf{s}, f)$	Coherence between gust velocity component i at \mathbf{p} and component j of the normalwash at \mathbf{s}
$\Lambda_{ij0n}(f)$	Coherence between gust velocity component i at the probe and normalwash component j at panel n
μ	Parameter used in analytical forms of $\psi_{ij}(\eta, \kappa)$ for Dryden and von Karman spectral models
ρ_{ij}	Correlation coefficient between responses due to gust components i and j
σ	RMS response amplitude
σ_i	RMS response amplitude due to gust component i
τ	Time lag
$\phi(f)$	$= 2 \int C(\tau) e^{-2\pi i f \tau} d\tau$ = Power spectrum of a dynamic response
$\phi_i(f)$	Cross spectrum between a dynamic response and gust velocity component i at the probe
$\varphi_i(\kappa)$	Nondimensional power spectrum of gust velocity component i
$\Phi(\mathbf{r}, f)$	$= 2 \int \mathbf{R}(\mathbf{r} + \mathbf{U}\tau, 0) e^{-2\pi i f \tau} d\tau$ = Cross spectrum tensor between gust velocities separated by \mathbf{r} in the aircraft system

NOMENCLATURE (Continued)

Scalars, Vectors and Dyadics:

$\psi_{ij}(\eta, \kappa)$	Component ij of nondimensional coherence tensor between gust velocities in rotated aircraft system
$\Psi(\mathbf{r}, \mathbf{s}, f)$	Cross spectrum between normalwashes at aerodynamic surface points \mathbf{r} and \mathbf{s}
$\Psi_{mn}(f)$	Cross spectrum between normalwashes at panels m and n
Ω	Wave number vector

Operational Symbols:

(\wedge)	Vector projection onto the plane $x = 0$
(\prime)	Vector reflection through the plane $y = 0$
$(\bar{})$	Vector or tensor transformation to the rotated aircraft system and (if frequency-dependent) referenced in phase to the plane $x = 0$
\cdot	Dot product between vectors
\times	Cross product between vectors
∇	Gradient operator in wave number space
(\sim)	Frequency-dependent quantity referenced in phase to the plane $x = 0$
\int	Full range integration unless limits are specified

NOMENCLATURE (Continued)

Operational Symbols:

$\langle \rangle$ Time average

$\delta(x) = (1/2\pi) \int e^{-ix\tau} d\tau =$ Dirac delta function

ϵ_i Sign indicator associated with definition of $\Lambda_{ij}(p, s, f)$

Matrix Notation:

$\{ \}$ Column matrix

$[]$ Rectangular matrix

$\lceil \rceil$ Diagonal matrix

$\{ \}^T, []^T$ Transposed matrix

$[]^{-1}$ Inverted matrix

$[\bar{\ }]$ Matrix transformed to modal coordinates

Matrix Root Symbols:

A Influence coefficient relating aerodynamic load without control system to gust normalwash or structural deflection

B Influence coefficient relating generalized input load to modal amplitude

D Influence coefficient relating total load to structural deflection

NOMENCLATURE (Continued)

Matrix Root Symbols:

g	Modal structural damping coefficient
G	Influence coefficient relating total load to gust normalwash
H	Frequency response function
I	Identity matrix
K	Stiffness
K'	Stiffness associated with elastic response load to be computed
L	Load
L'	Load response to be computed
M	Mass
q	Modal amplitude
Q	Generalized load
S	Influence coefficient relating aerodynamic load due to control system action to gust normalwash or structural deflection
w	Gust normalwash
X	Structural deflection

NOMENCLATURE (Continued)

Matrix Root Symbols:

ϕ	Cross spectrum between structural responses
Φ	Mode shape
Ψ	Normalwash cross spectrum
ω	Angular frequency
$\bar{\omega}$	Modal eigenfrequency

Subscripts and Superscripts:

E	Elastic response
L	Load response to be computed
q	Modal amplitude
R	Rigid body response
w	Gust normalwash
X	Structural deflection
+	Symmetric with respect to the plane $y = 0$
-	Antisymmetric with respect to the plane $y = 0$
*	Complex conjugate

Contrails

SECTION I

INTRODUCTION

The development of aircraft of increasing size and flexibility has stimulated renewed interest in the problem of representing the full three-dimensional spatial dependence of the turbulence field in gust design calculations. This may be contrasted with conventional design procedures which treat vertical and lateral gusts separately and allow them to vary only along the axial (x) direction in accordance with the one-dimensional turbulence assumption. Thus, variations with transverse (y, z) position are ignored, and the turbulence velocity is assumed to be uniform throughout any plane normal to the flight path. This approximation may result in errors in dynamic load calculations if the transverse dimensions of the aircraft are not small compared to spatial wavelengths that are capable of exciting significant structural responses. Furthermore, the analytical substantiation of spectral relationships between structural responses and probe-measured gust velocities obtained from dynamic response tests may be hampered, particularly at the higher flexible response frequencies.

Treatment of the multi-dimensional gust response problem has largely proceeded along two independent but mathematically equivalent courses. The first approach was originated by Liepmann (Reference 1) and extended by Ribner (Reference 2). It requires that the frequency response function of the structure be expressed in the wave domain. Since this is usually difficult, the method is applicable in its basic form only to the simplest configurations.

Contrails

A modification developed by Etkin (Reference 3) and elaborated in Reference 4 has more general application, but involves a power series expansion which is subject to divergence.

The second approach, originated by Diederich (Reference 5), utilizes the frequency response function in the original space domain, but generally requires the evaluation of a large quadratic form to obtain the response power spectrum in accordance with multiple input procedures. The two-dimensional version of this method is exemplified by Reference 6 and 7, and corresponds to the rudimentary case of a flat aircraft responding only to vertical gust. Lateral gust response must be treated separately in this case. A 3-D version is proposed for general configurations in Reference 8, but the turbulence description which is provided is limited to the 2-D case.

The first complete three-dimensional formulation of the space domain approach for general configurations is contained in Reference 9. A unified theory is derived which describes the dynamic response of a flexible aircraft traversing a random, isotropic field of atmospheric turbulence. The formulation not only assigns full three-dimensional spatial dependence to all three direction components of the gust velocity, but departs from the conventional space domain approach by decomposing the incremental turbulence velocity field into two statistically independent subfields, one symmetric and the other antisymmetric with respect to the midplane of the aircraft. All of the mathematical redundancies attributable to the conventional approach are subsequently eliminated, thereby reducing the size of the multiple input calculation by a factor

Contrails

of 36. By this means, variation of the gust with transverse position can be economically treated in the analysis of large aircraft, and responses to more than one gust direction may be rationally combined into a single calculation. Furthermore, the theory and methods may be extended to include the analytical counterparts of the various frequency-dependent functions normally obtained by spectral analysis of data derived from dynamic response tests in which a gust probe is employed. These include: (1) response power spectra and transfer functions, which require application of power spectral methods, and (2) cross-transfer functions and coherence functions, which require the additional application of cross-spectral techniques.

The new method is fully compatible with current gust criteria and utilizes gust input power spectra and frequency response functions identical to those in the one-dimensional case, except that the gust reference direction is chosen normal to each input panel rather than parallel to the x, y and z axes of the aircraft coordinate system. It is even trivially possible to reduce the analysis to any number of rudimentary or degenerate cases such as those described above, although there is usually little computational advantage in this. It is easily shown that if the transverse dimensions of the aircraft are sufficiently small, then the calculated results of the 3-D gust response model approach identically the conventional 1-D analysis.

SECTION II

TECHNICAL BACKGROUND

The theory of three-dimensional gust response is developed in this section and in Reference 9 as a nonredundant extension of the space domain formulation. An alternative approach, termed the wave domain formulation, is mathematically equivalent to the first and may be derived from it by multiple Fourier transformation. However, difficulties exist in its practical application which are described in Appendix A, where a detailed mathematical derivation of both general formulations is furnished, and the underlying assumptions concerning the physical properties of atmospheric turbulence are introduced.

2.1 FREQUENCY RESPONSE FUNCTIONS

The frequency response function for a structure may be written $H(\mathbf{r}, f)$, and represents the complex amplitude ratio between a given structural response and a simple harmonic excitation $e^{i\omega t}$ applied at point \mathbf{r} of the structure, where $f = \omega/2\pi$ denotes the excitation frequency. The excitation is here taken to be a normal-wash of unit amplitude impinging upon a unit aerodynamic surface at \mathbf{r} .

It is often convenient to reference the phase of the frequency response function to the input point $\hat{\mathbf{r}} = (0, r_2, r_3)$ corresponding to the projection of $\mathbf{r} = (r_1, r_2, r_3)$ onto the plane $x = 0$ of a reference system moving with the aircraft. This is accomplished

Contrails

by inserting the phase delay factor $e^{-i\omega r_1/U}$, where the velocity of the aircraft is taken as $\mathbf{U} = (-U, 0, 0)$ with respect to a fixed reference system. Then

$$\tilde{H}(\mathbf{r}, f) = e^{-i\omega r_1/U} H(\mathbf{r}, f) \quad (2.1)$$

where the tilde signifies that the phase is referenced to the plane $x = 0$ of the aircraft system. Since an aircraft is usually a bilaterally symmetric structure, it is also customary to employ frequency response functions corresponding to symmetric (+) and antisymmetric (-) input configurations. If a prime is used to denote reflection of a vector through the plane $y = 0$, then the two input configurations correspond to unit inputs simultaneously applied at \mathbf{r} and \mathbf{r}' along the normalwash directions represented by the unit vectors $\mathbf{n}(\mathbf{r})$ and $\mathbf{n}(\mathbf{r}')$ shown in Figure 1. The resulting frequency response functions are then given by

$$\tilde{H}^{\pm}(\mathbf{r}, f) = \tilde{H}(\mathbf{r}, f) \pm \tilde{H}(\mathbf{r}', f) \quad (2.2)$$

Naturally, symmetric and antisymmetric input configurations tend to excite responses of corresponding symmetry only. The total response of the structure is obtained by superimposing the symmetric and antisymmetric responses.

2.2 THREE-DIMENSIONAL TURBULENCE

The three-dimensional gust velocity field may be resolved into two independent subfields, one symmetric, and the other antisymmetric with respect to the midplane of the aircraft. The

Contrails

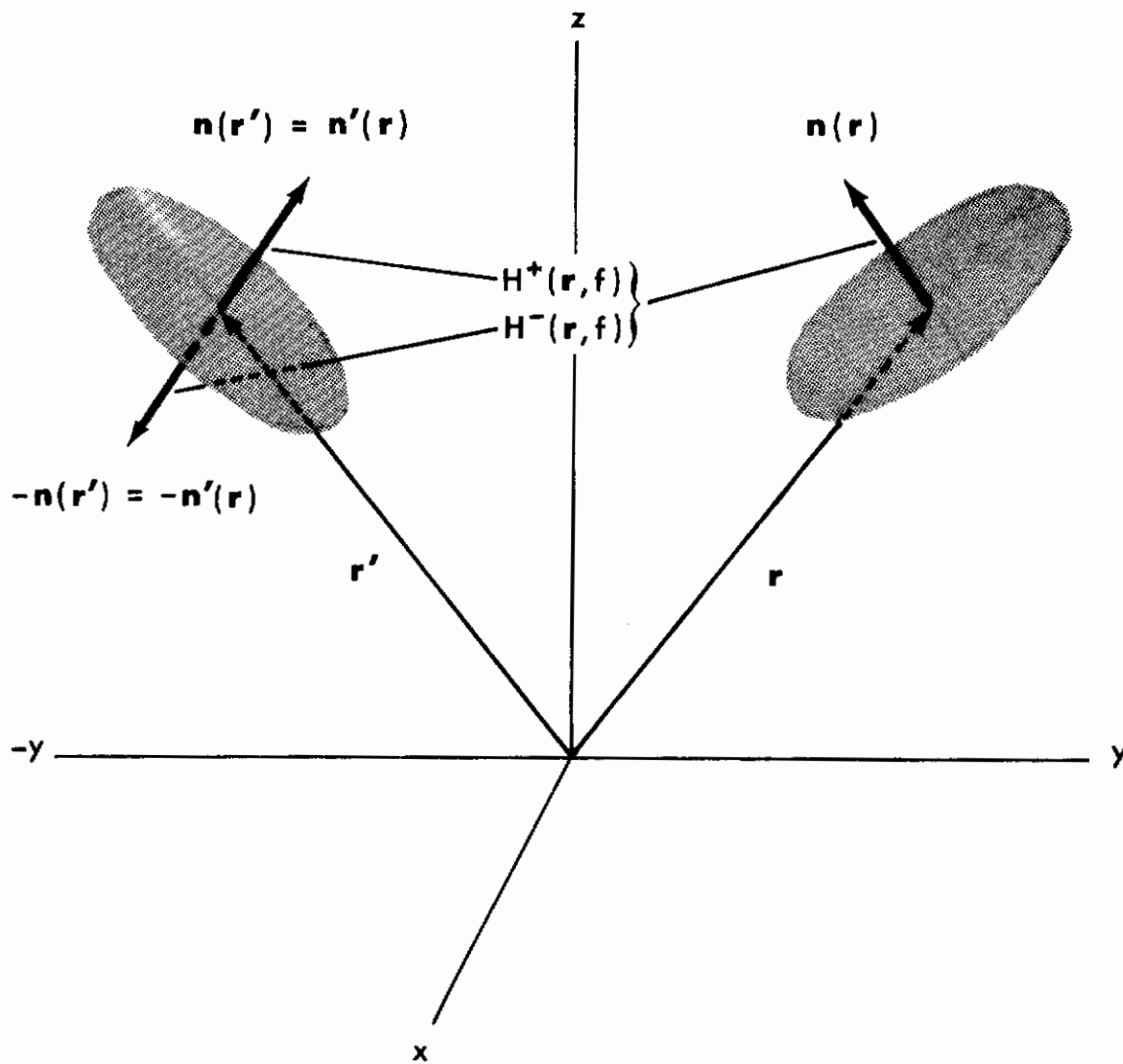


Figure 1. Unit Directional Vector Pairs Corresponding to Symmetric (+) and Antisymmetric (-) Normalwash Input Configurations

Contrails

subfields have the useful property of selectively exciting only symmetric and antisymmetric responses, respectively. This procedure ultimately results in a considerable simplification of the response analysis according to the method of Reference 2.

Let $\mathbf{u}(\mathbf{r},t)$ represent the gust velocity at point \mathbf{r} and time t . Employing the primed vector notation to denote reflection through the plane $y = 0$, the symmetric (+) and antisymmetric (-) subfields are given by

$$\mathbf{u}^{\pm}(\mathbf{r},t) = [\mathbf{u}(\mathbf{r},t) \pm \mathbf{u}'(\mathbf{r}',t)] / 2 \quad (2.3)$$

A geometrical construction illustrating the decomposition process is shown in Figure 2. The original gust velocity distribution is restored by superimposing the respective subfields. Thus,

$$\mathbf{u}(\mathbf{r},t) = \mathbf{u}^{+}(\mathbf{r},t) + \mathbf{u}^{-}(\mathbf{r},t) \quad (2.4)$$

Figure 3 shows the result of applying the decomposition process of equation (2.3) to an assumed three-dimensional gust velocity distribution. The coordinate system used in the decomposition is that of the aircraft shown in silhouette. A front view has been chosen for simplicity. Consequently, the longitudinal component of turbulence is not visible. Notice that the gust input distributions resulting from the symmetric and antisymmetric subfields, are such as to induce aircraft responses that are correspondingly symmetric and antisymmetric, respectively. Furthermore, we see that symmetric and antisymmetric responses are induced by both vertical and lateral gust inputs in the 3-D turbulence description.

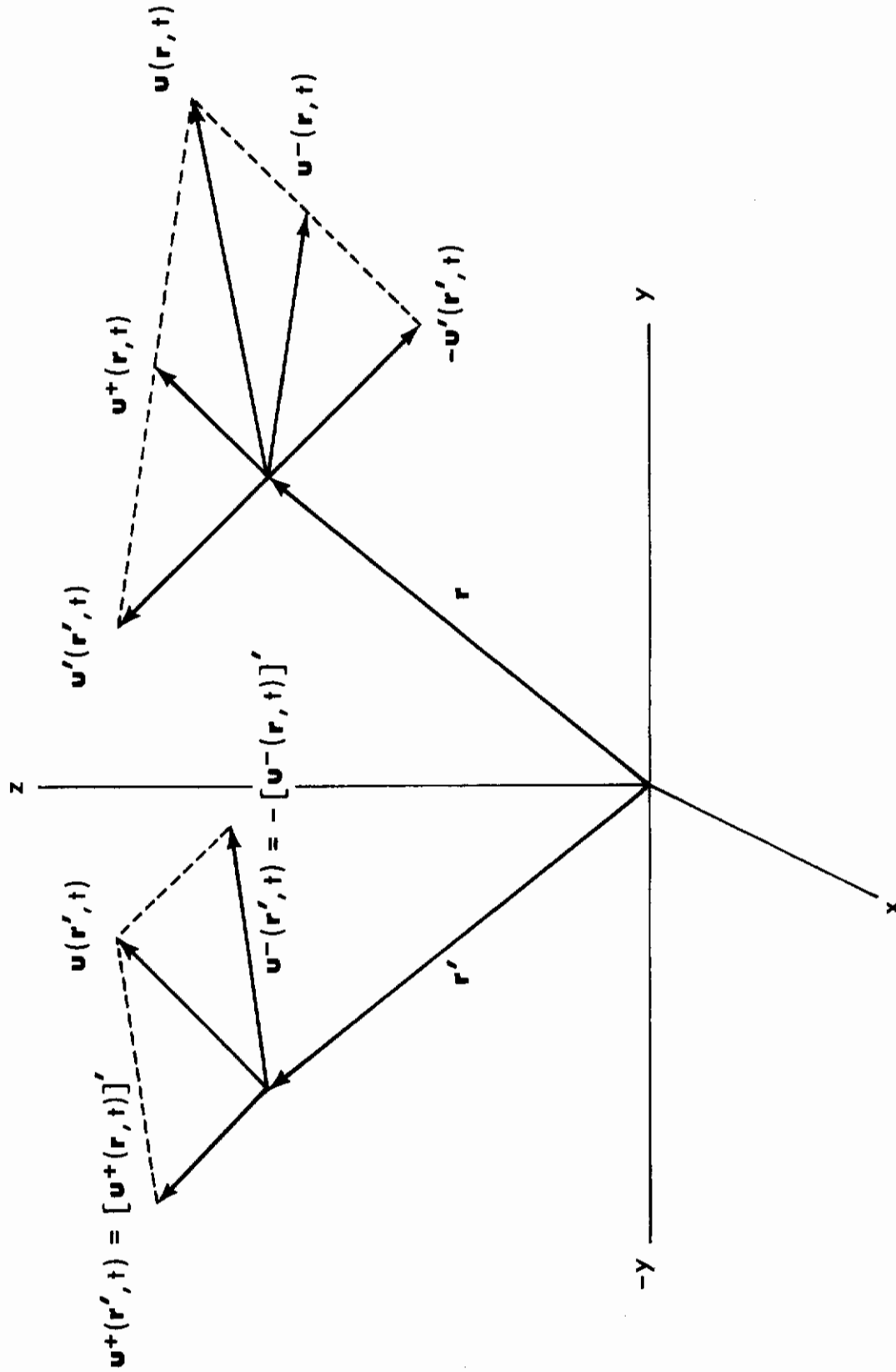


Figure 2. Resolution of Gust Velocity into Symmetric (+) and Antisymmetric (-) Subfields

TOTAL 3-D GUST VELOCITY

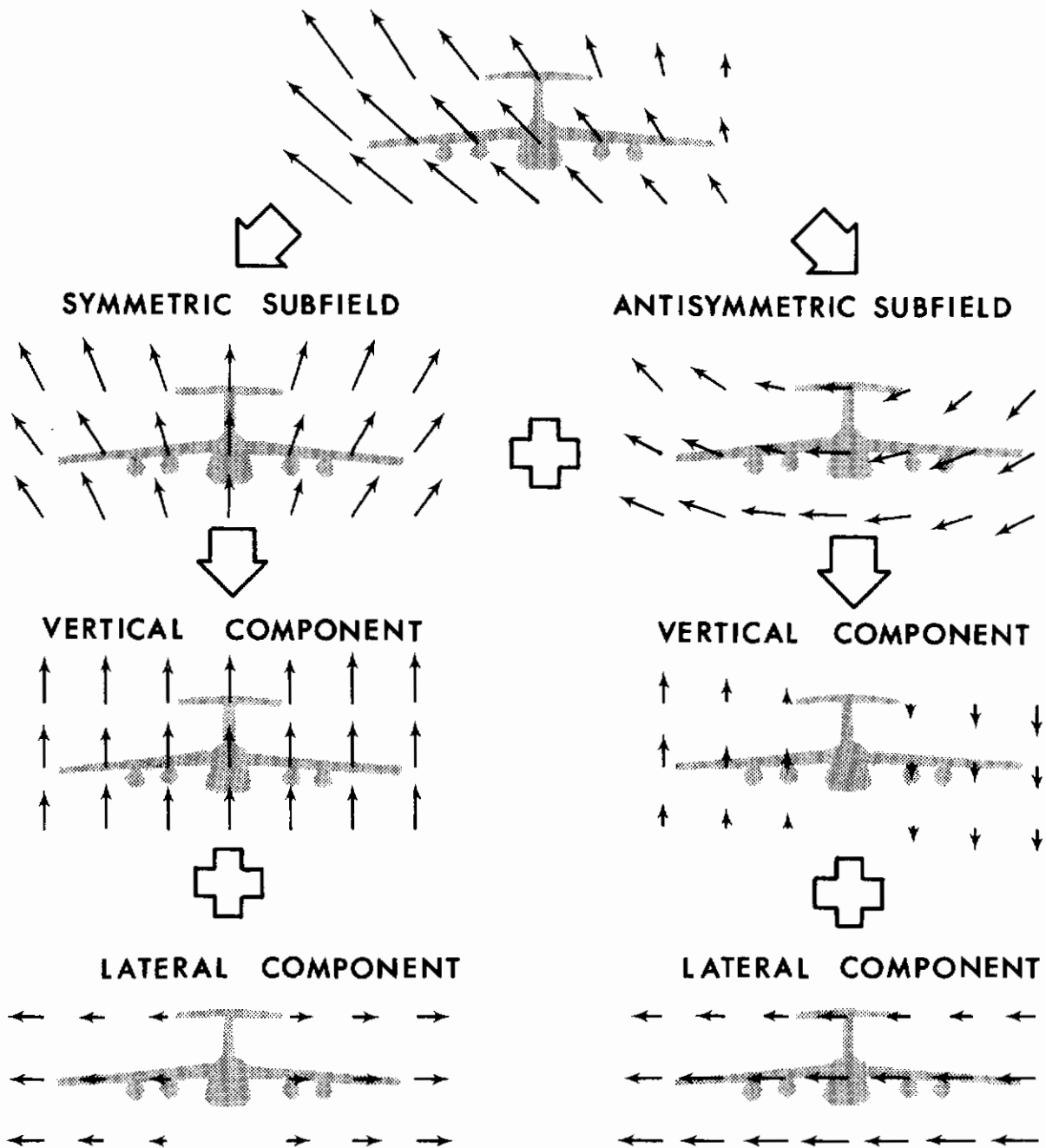


Figure 3. Decomposition of a Three-Dimensional Turbulence Velocity Field

Contrails

The dimensionality of the turbulence description refers to the number of position coordinates upon which the gust velocity is assumed to depend. The usual convention is given by

$$\mathbf{u}(\mathbf{r}, t) = \begin{cases} \mathbf{u}(t) & 0\text{-D} \\ \mathbf{u}(x, t) & 1\text{-D} \\ \mathbf{u}(x, y, t) & 2\text{-D} \\ \mathbf{u}(x, y, z, t) & 3\text{-D} \end{cases} \quad (2.5)$$

Less common 1-D descriptions involve replacement of x by y or z . Similarly, by replacing x, y by y, z or x, z , the remaining 2-D descriptions are obtained. It is important to recognize that the dimensionality of the turbulence field does not depend upon the number or identity of gust velocity direction components, u_1, u_2 or u_3 , which may be included in the aircraft response description.

Figure 4 shows the result of applying the decomposition process to the conventional 2-D turbulence description of equation (2.5). Notice that the resulting turbulence field permits no gust variation relative to vertical position and is rigorously applicable only to aircraft whose aerodynamic surfaces are coplanar. Consequently, in a strict sense the 2-D gust model is not appropriate to the T-tail aircraft shown in the figure.

Figure 5 shows the result of applying the decomposition process to the conventional 1-D gust model of equation (2.5). Notice that no gust variation relative to either vertical or lateral position is permitted. Furthermore, vertical gusts excite only symmetric responses and lateral gusts excite only antisymmetric responses, in agreement with current 1-D analysis procedures.

TOTAL 2-D GUST VELOCITY

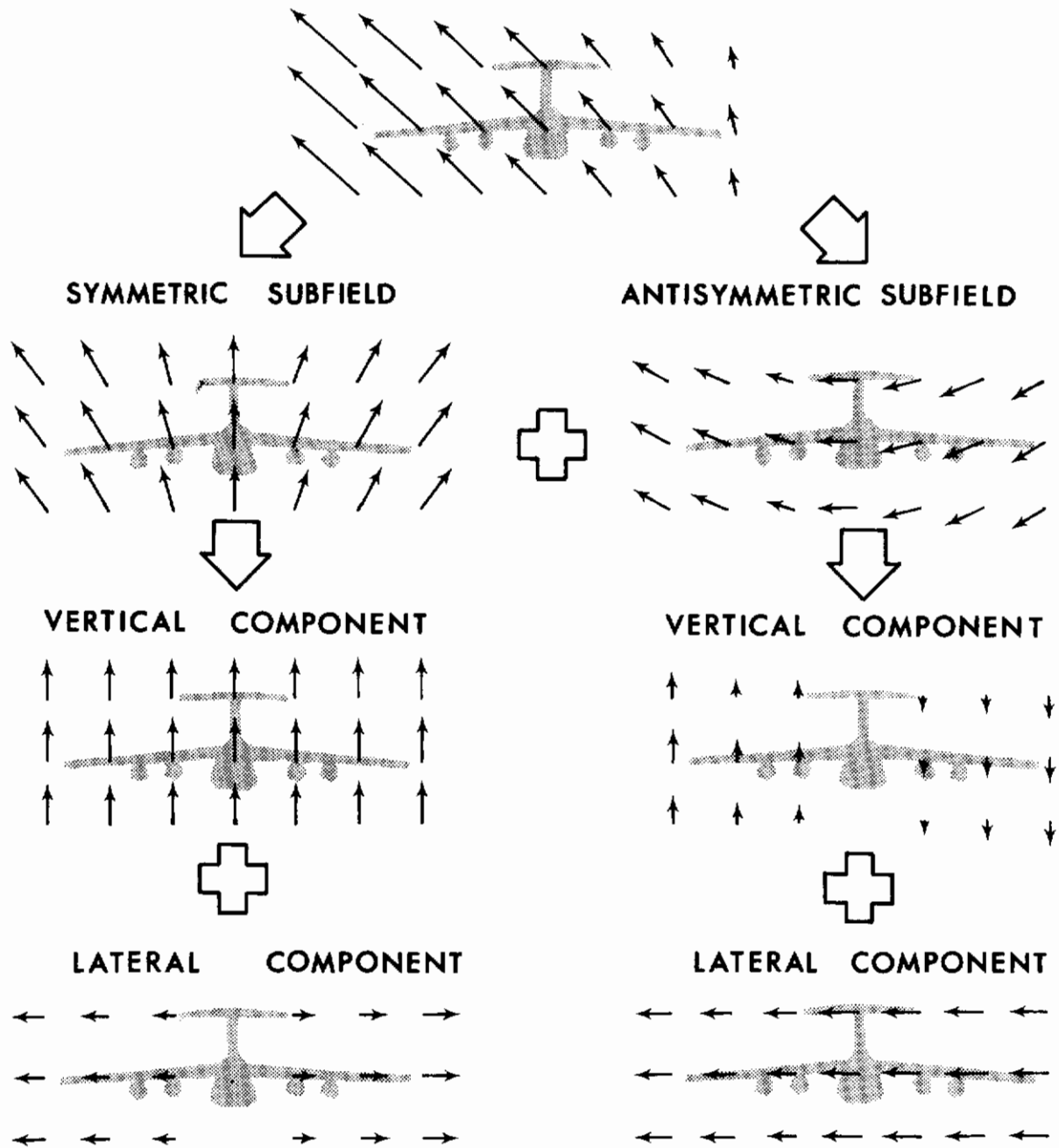


Figure 4. Decomposition of a Two-Dimensional Turbulence Velocity Field

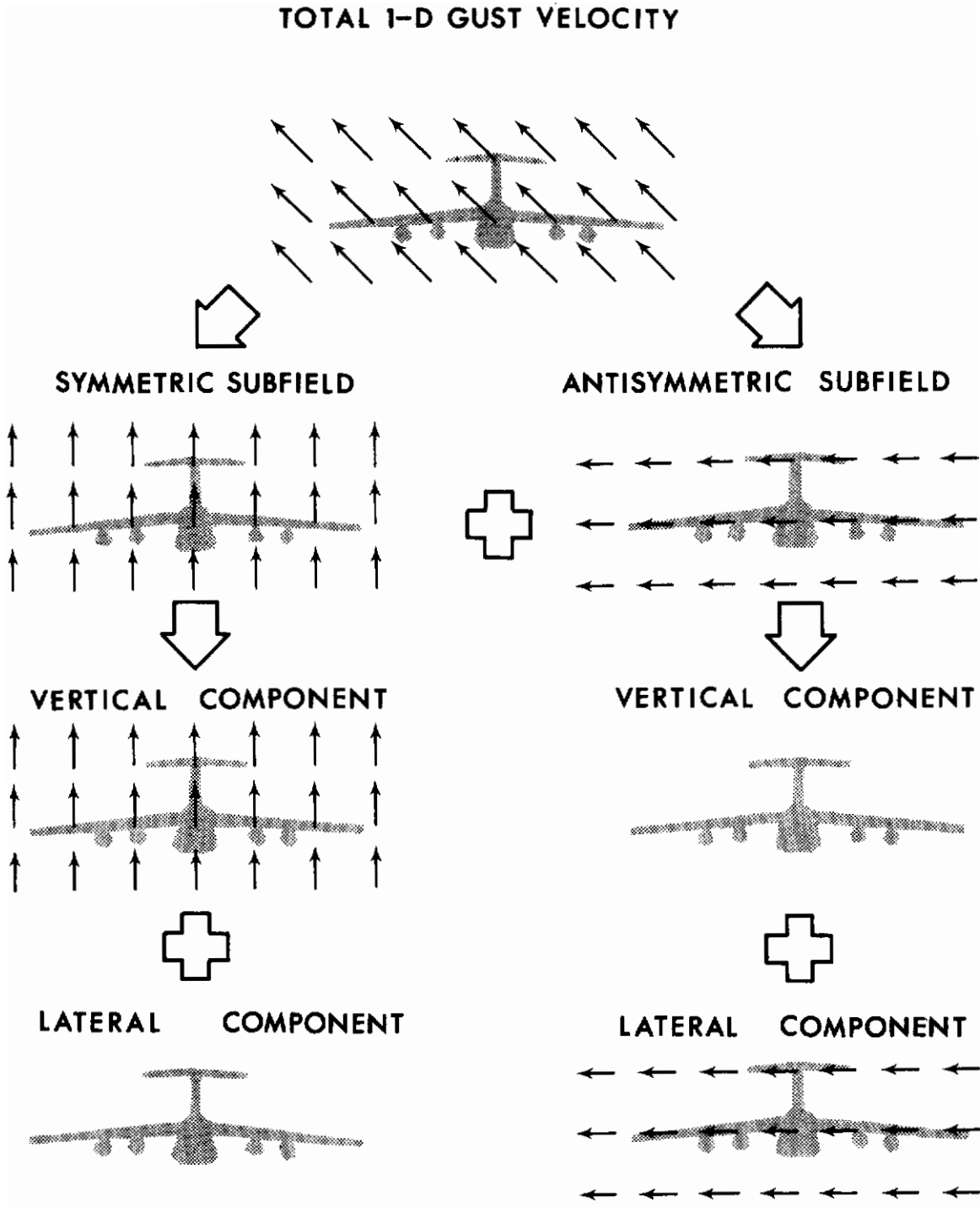


Figure 5. Decomposition of a One-Dimensional Turbulence Velocity Field

2.3 NONREDUNDANT SPACE DOMAIN FORMULATION

The response power spectra, $\phi(f)$, contain the essential information required to evaluate the gust response of an aircraft. According to the space domain formulation derived as equation (A-5) of Appendix A,

$$\phi(f) = \int \mathbf{H}^*(\mathbf{r}, f) \cdot \Phi(\mathbf{s} - \mathbf{r}, f) \cdot \mathbf{H}(\mathbf{s}, f) d\mathbf{r} d\mathbf{s} \quad (2.6)$$

where $\Phi = \Phi_{11} \mathbf{i} \mathbf{i} + \Phi_{22} \mathbf{j} \mathbf{j} + \Phi_{33} \mathbf{k} \mathbf{k} + \Phi_{12} (\mathbf{i} \mathbf{j} + \mathbf{j} \mathbf{i}) + \Phi_{13} (\mathbf{i} \mathbf{k} + \mathbf{k} \mathbf{i}) + \Phi_{23} (\mathbf{j} \mathbf{k} + \mathbf{k} \mathbf{j})$

The integrations indicated above are performed over the aerodynamic surfaces, and the asterisk denotes the complex conjugate. $\mathbf{H}(\mathbf{r}, f)$ is the vector frequency response function whose components represent the responses to unit backwash, sidewash and upwash, respectively. The nine-component cross spectrum tensor, $\Phi(\mathbf{s} - \mathbf{r}, f)$, between gust velocities measured at the two input points is written as a dyadic to permit the familiar methods of vector manipulation to be employed. The dot symbol signifies scalar multiplication, so that the indicated pre- and post- multiplication of the cross spectrum dyadic by the vector frequency response function results in a scalar integrand.

Equation (2.6) can be reduced to nonredundant form by following the procedure derived in Reference 9. To begin with, the definition of $\mathbf{H}(\mathbf{r}, f)$ in Paragraph 2.1 implies that

$$\mathbf{H}(\mathbf{r}, f) = H(\mathbf{r}, f) \mathbf{n}(\mathbf{r}) \quad (2.7)$$

where $H(\mathbf{r}, f)$ is the frequency response function associated with normalwash, and $\mathbf{n}(\mathbf{r})$ is the unit vector in the normalwash direction.

Substituting this result into equation (2.6) yields

$$\phi(f) = \int H^*(\mathbf{r}, f) \Psi(\mathbf{r}, \mathbf{s}, f) H(\mathbf{s}, f) d\mathbf{r} d\mathbf{s} \quad (2.8)$$

where $\Psi(\mathbf{r}, \mathbf{s}, f) = \mathbf{n}(\mathbf{r}) \cdot \Phi(\mathbf{s} - \mathbf{r}, f) \cdot \mathbf{n}(\mathbf{s})$

Ψ is the gust normalwash cross spectrum, since it represents the cross spectrum between those components of the gust velocity which are measured in the normalwash directions at the two input points. Equation (2.8) achieves a nine-fold reduction in computational effort, since the integrand contains one term as compared to nine in equation (2.6).

Further simplification is gained by introducing the frequency response function whose phase is referenced to the projected input point according to equation (2.1). Since the corresponding gust normalwash cross spectrum must also be referenced in phase to the plane $x = 0$, the associated gust velocity cross spectrum tensor is no longer a function of the longitudinal separation between input points, so that

$$\phi(f) = \int \tilde{H}^*(\mathbf{r}, f) \tilde{\Psi}(\mathbf{r}, \mathbf{s}, f) \tilde{H}(\mathbf{s}, f) d\mathbf{r} d\mathbf{s} \quad (2.9)$$

where $\tilde{\Psi}(\mathbf{r}, \mathbf{s}, f) = \mathbf{n}(\mathbf{r}) \cdot \Phi(\hat{\mathbf{s}} - \hat{\mathbf{r}}, f) \cdot \mathbf{n}(\mathbf{s})$

The gust velocity cross spectrum tensor can be further reduced by expressing it in a new reference frame obtained by rotating the aircraft coordinate system about the x axis so that the new y axis is parallel to $\hat{\mathbf{s}} - \hat{\mathbf{r}}$, as illustrated in Figure 6. The vertical component of the transverse separation vector is eliminated by the rotation, leaving only a lateral separation of magnitude $|\hat{\mathbf{s}} - \hat{\mathbf{r}}|$ in

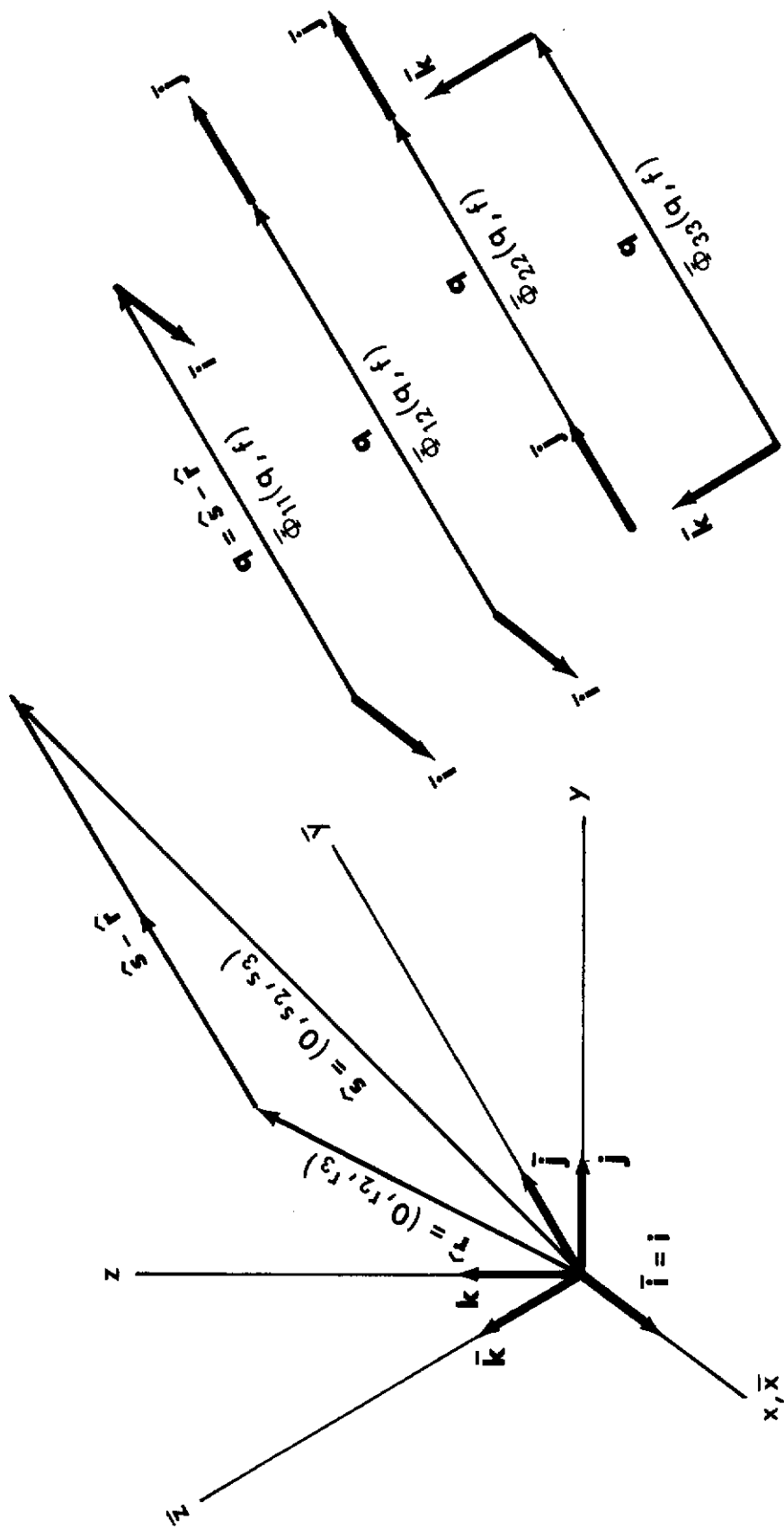


Figure 6. Representation of the Gust Velocity Cross Spectrum Tensor in the Rotated Coordinate System

the new coordinate system. Displaying the spatial variables explicitly and denoting the new coordinate vectors and the representation of the tensor in the new reference frame by an overbar, we obtain

$$\Phi(0, y, z, f) = \bar{\Phi}(0, q, 0, f) \quad (2.10)$$

where $\bar{\Phi} = \bar{\Phi}_{11} \bar{\mathbf{i}}\bar{\mathbf{i}} + \bar{\Phi}_{22} \bar{\mathbf{j}}\bar{\mathbf{j}} + \bar{\Phi}_{33} \bar{\mathbf{k}}\bar{\mathbf{k}} + \bar{\Phi}_{12} (\bar{\mathbf{i}}\bar{\mathbf{j}} + \bar{\mathbf{j}}\bar{\mathbf{i}})$

and $y = s_2 - r_2, z = s_3 - r_3, q = (y^2 + z^2)^{1/2}$

We note that the tensor reduces to only four distinct non-zero components in the new reference frame. These components correspond to the four basic velocity configurations shown in the figure and are functions of only two scalar quantities: the frequency, f , and the transverse separation between input points, q . Analytical expressions for the four tensor components are derivable for any of the common isotropic turbulence models such as the Dryden or von Karman. A detailed discussion of their properties is presented in Section IV. The coordinate vectors of the rotated reference system are given by

$$\begin{aligned} \bar{\mathbf{i}} &= \mathbf{i} & \bar{\mathbf{j}} &= (\hat{\mathbf{s}} - \hat{\mathbf{r}})/|\hat{\mathbf{s}} - \hat{\mathbf{r}}| & \bar{\mathbf{k}} &= \bar{\mathbf{i}} \times \bar{\mathbf{j}} \\ & & &= (y\mathbf{j} + z\mathbf{k})/q & &= (-z\mathbf{j} + y\mathbf{k})/q \end{aligned} \quad (2.11)$$

and the Cartesian components of $\mathbf{n}(\mathbf{r})$ can be written

$$n_1(\mathbf{r}) = \mathbf{n}(\mathbf{r}) \cdot \mathbf{i} \quad n_2(\mathbf{r}) = \mathbf{n}(\mathbf{r}) \cdot \mathbf{j} \quad n_3(\mathbf{r}) = \mathbf{n}(\mathbf{r}) \cdot \mathbf{k} \quad (2.12)$$

For an input point \mathbf{r}' in the negative y half-space, one may observe that $r'_2 = -r_2$ and $n_2(\mathbf{r}') = -n_2(\mathbf{r})$. The remaining components

Contrails

of the normalwash vectors at \mathbf{r} and \mathbf{r}' are identical, since the aircraft is symmetric about the plane $y = 0$.

Substituting equations (2.10) through (2.12) into the expression for the gust normalwash cross spectrum in (2.9) yields

$$\begin{aligned} \tilde{\Psi}(\mathbf{r}, \mathbf{s}, f) = & \bar{\Phi}_{11}(q, f) n_1(\mathbf{r}) n_2(\mathbf{s}) + \\ & [\bar{\Phi}_{22}(q, f) - \bar{\Phi}_{33}(q, f)] [y n_2(\mathbf{r}) + z n_3(\mathbf{r})] [y n_2(\mathbf{s}) + z n_3(\mathbf{s})] / q^2 + \\ & \bar{\Phi}_{33}(q, f) [n_2(\mathbf{r}) n_2(\mathbf{s}) + n_3(\mathbf{r}) n_3(\mathbf{s})] + \\ & \bar{\Phi}_{12}(q, f) \left\{ n_1(\mathbf{r}) [y n_2(\mathbf{s}) + z n_3(\mathbf{s})] + n_1(\mathbf{s}) [y n_2(\mathbf{r}) + z n_3(\mathbf{r})] \right\} / q \end{aligned} \quad (2.13)$$

where $y = s_2 - r_2$, $z = s_3 - r_3$, $q = (y^2 + z^2)^{1/2}$

The next reduction of the space domain formulation is accomplished by introducing into equation (2.9) the frequency response functions defined by equation (2.2) and illustrated by Figure 1. Although these functions are referred to a single input point \mathbf{r} , they are associated with symmetric and antisymmetric input configurations which include \mathbf{r}' , so that the double surface integral may be confined to one side of the $y = 0$ plane of symmetry. This will be indicated by restricting the region of integration to $r_2, s_2 > 0$. The net reduction in computation is two-fold, since the two symmetries must be treated separately.

The symbol $\tilde{\Psi}^{\pm}$ will denote the gust normalwash cross spectra associated with symmetric (+) and antisymmetric (-) input configurations. Each is equal to the sum of the four ordinary gust normalwash cross spectra which relate the gust normalwashes between single points belonging to input configurations of like

symmetry, as shown in Figure 7. Then

$$\begin{aligned} \tilde{\Psi}^{\pm}(\mathbf{r}, \mathbf{s}, f) &= [\tilde{\Psi}(\mathbf{r}, \mathbf{s}, f) + \tilde{\Psi}(\mathbf{r}', \mathbf{s}', f) \pm \tilde{\Psi}(\mathbf{r}', \mathbf{s}, f) \pm \tilde{\Psi}(\mathbf{r}, \mathbf{s}', f)]/4 \\ &= [\tilde{\Psi}(\mathbf{r}, \mathbf{s}, f) \pm \tilde{\Psi}(\mathbf{r}', \mathbf{s}, f)]/2 \end{aligned} \quad (2.14)$$

where division by four accounts for the fact that only half of the gust velocity configuration for each symmetry is available according to equation (2.3). It may be deduced from symmetry considerations that equalities exist among the four ordinary cross spectra in equation (2.14), such that they may be combined and reduced to two, as shown.

When the above substitutions have been made, equation (2.9) may be replaced by

$$\phi(f) = \phi^{+}(f) + \phi^{-}(f) \quad (2.15)$$

$$\text{where } \phi^{\pm}(f) = \int_{r_2, s_2 > 0} \tilde{H}^{\pm*}(\mathbf{r}, f) \tilde{\Psi}^{\pm}(\mathbf{r}, \mathbf{s}, f) \tilde{H}^{\pm}(\mathbf{s}, f) d\mathbf{r} d\mathbf{s}$$

2.4 PANEL SUMMATION FORM

A further two-fold reduction in computation can be derived from the fact that interchanging the input points in the integrand of equation (2.15) is equivalent to replacing the integrand by its complex conjugate. However, since the result is awkward to express as a continuous integral, it is expedient at this point to pass to the panel summation form of equation (2.15) by defining the discrete frequency response functions

$$H_m^{\pm}(f) = \int_{\text{panel } m} \tilde{H}^{\pm}(\mathbf{r}, f) d\mathbf{r} \quad m = 1, \dots, N \quad (2.16)$$

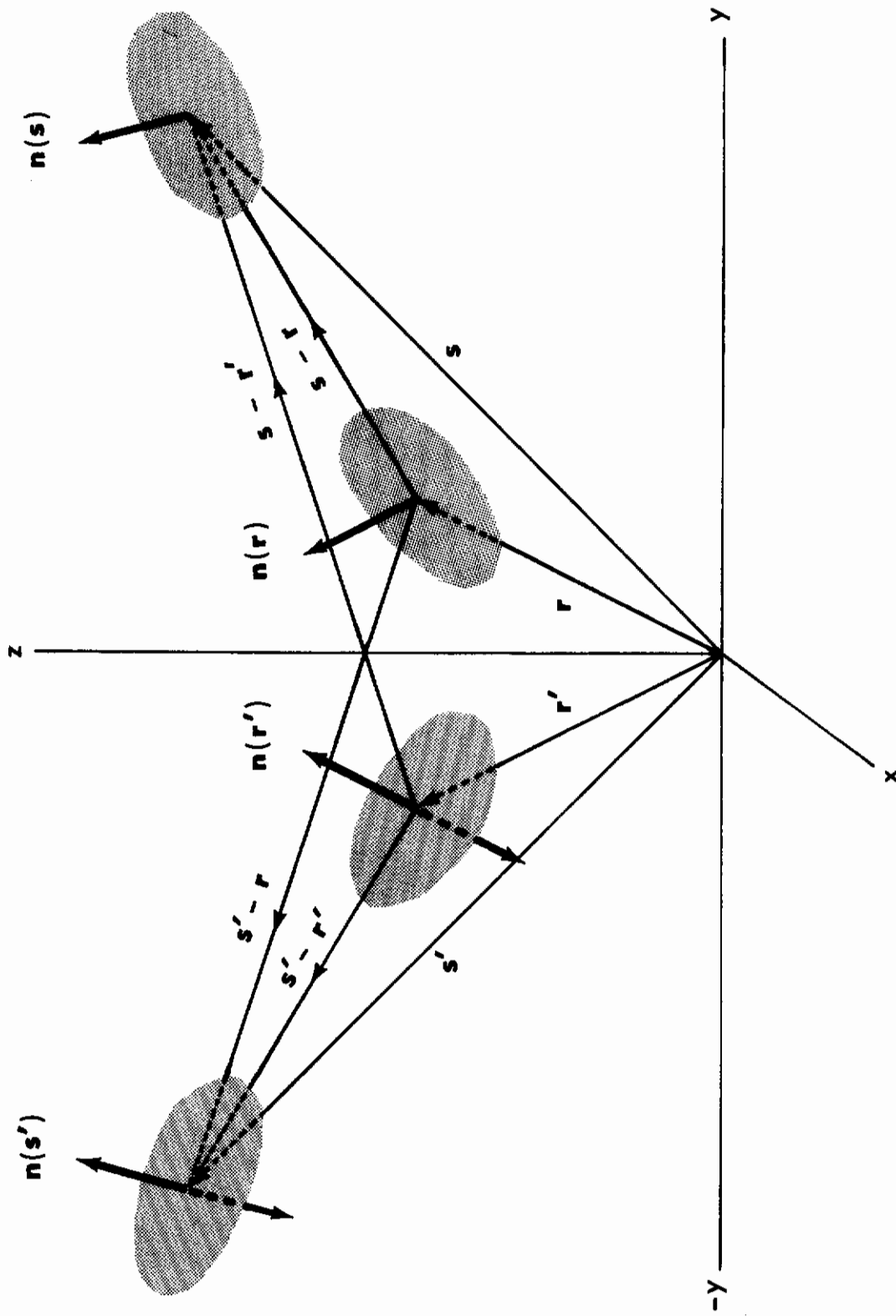


Figure 7. Normalwash Input Configurations for Calculating Symmetric and Antisymmetric Normalwash Cross Spectra

where N is the total number of symmetrically located pairs of aerodynamic surface panels into which the aircraft has been divided for computation. The corresponding gust normalwash cross spectra depend upon panel pairs m and n , whose positive y members are assumed to be located at \mathbf{r} and \mathbf{s} , respectively.

$$\Psi_{mn}^{\pm}(f) = \tilde{\Psi}^{\pm}(\mathbf{r}, \mathbf{s}, f) \quad (2.17)$$

Applying these definitions to the integral formulation and suppressing the frequency variable for brevity yields

$$\begin{aligned} \phi^{\pm} &= \sum_{n=1}^N \sum_{m=1}^N H_m^{\pm*} \Psi_{mn}^{\pm} H_n^{\pm} = \sum_{n=1}^N \left[|H_n^{\pm}|^2 \Psi_{nn}^{\pm} + \sum_{m=1}^{n-1} (H_m^{\pm*} \Psi_{mn}^{\pm} H_n^{\pm} + H_m^{\pm} \Psi_{mn}^{\pm*} H_n^{\pm*}) \right] \\ &= \sum_{n=1}^N \left\{ |H_n^{\pm}|^2 \Psi_{nn}^{\pm} + 2 \sum_{m=1}^{n-1} [\operatorname{Re}(H_m^{\pm*} H_n^{\pm}) \operatorname{Re}(\Psi_{mn}^{\pm}) - \operatorname{Im}(H_m^{\pm*} H_n^{\pm}) \operatorname{Im}(\Psi_{mn}^{\pm})] \right\} \quad (2.18) \end{aligned}$$

2.5 GUST VELOCITY COHERENCE TENSOR

The gust velocity coherence tensor, Γ , is defined by normalizing each component of the gust velocity cross spectrum tensor in the fashion:

$$\Gamma_{ij}(\mathbf{r}, f) = \Phi_{ij}(\mathbf{r}, f) / [\Phi_i(f) \Phi_j(f)]^{1/2} \quad (2.19)$$

where $\Phi_i(f) = \Phi_{ii}(\mathbf{0}, f)$

Φ_i is the power spectrum of the i th gust velocity component, since it represents the cross spectrum between like Cartesian components at zero separation distance. According to equation (2.19),

$$\Phi_{ij}(\mathbf{r}, f) = \Gamma_{ij}(\mathbf{r}, f) [\Phi_i(f) \Phi_j(f)]^{1/2} \quad (2.20)$$

Thus, each component of Γ serves to separate the coherence and power spectral characteristics of the corresponding component of Φ into two factors. Moreover, since the convenient tensor transformation properties described by equation (2.10) hold for Γ as well as Φ , by applying (2.11) and (2.12), we obtain

$$\Gamma(\mathbf{s} - \mathbf{r}, f) = \bar{\Gamma}(q, f) \quad (2.21)$$

where

$$\begin{aligned} \Gamma_{11} &= \bar{\Gamma}_{11}, \quad \Gamma_{22} = \bar{\Gamma}_{33} + (y/q)^2 (\bar{\Gamma}_{22} - \bar{\Gamma}_{33}), \quad \Gamma_{33} = \bar{\Gamma}_{33} + (z/q)^2 (\bar{\Gamma}_{22} - \bar{\Gamma}_{33}) \\ \Gamma_{12} &= \Gamma_{21} = (y/q) \bar{\Gamma}_{12}, \quad \Gamma_{13} = \Gamma_{31} = (z/q) \bar{\Gamma}_{12}, \quad \Gamma_{23} = \Gamma_{32} = (yz/q^2) (\bar{\Gamma}_{22} - \bar{\Gamma}_{33}) \\ y &= s_2 - r_2, \quad z = s_3 - r_3, \quad q = (y^2 + z^2)^{1/2} \end{aligned}$$

Equation (2.20) is applied in Section IV to develop a convenient tabular procedure for evaluating the components of $\bar{\Phi}$ contained in equation (2.13). Equations (2.20) and (2.21) are utilized in Paragraphs 2.6 and 2.7 to define response transfer functions and cross transfer functions for the general case of three-dimensional turbulence. These functions are analogous to those which occur in one-dimensional gust response analysis and can be shown to reduce to them in the small aircraft limit (Reference 2).

2.6 TRANSFER FUNCTIONS

An alternative formulation of equation (2.15) may be derived which extends the concept of the conventional transfer function to three-dimensional gust response analysis. By analogy with equation (2.14), define symmetric and antisymmetric gust normalwash

coherence matrices

$$\tilde{\Theta}_{ij}^{\pm}(\mathbf{r}, \mathbf{s}, f) = [\tilde{\Theta}_{ij}^{\pm}(\mathbf{r}, \mathbf{s}, f) \pm \tilde{\Theta}_{ij}^{\pm}(\mathbf{r}', \mathbf{s}, f)]/2 \quad (2.22)$$

where $\tilde{\Theta}_{ij}^{\pm}(\mathbf{r}, \mathbf{s}, f) = n_i(\mathbf{r}) \Gamma_{ij}(\hat{\mathbf{s}} - \hat{\mathbf{r}}, f) n_j(\mathbf{s})$

$\tilde{\Theta}_{ij}^{\pm}(\mathbf{r}, \mathbf{s}, f)$ represents element ij of the gust normalwash coherence matrix, and equals the coherence between normalwash components i and j measured at \mathbf{r} and \mathbf{s} , respectively, and referenced in phase to the $x = 0$ plane. Substituting equation (2.22) into (2.15) yields

$$\phi^{\pm}(f) = \sum_{j=1}^3 \left\{ T_{jj}^{2\pm}(f) \Phi_j(f) + 2 \sum_{i=1}^{j-1} T_{ij}^{2\pm}(f) [\Phi_i(f) \Phi_j(f)]^{1/2} \right\} \quad (2.23)$$

where $T_{ij}^{2\pm}(f) = \int_{r_2, s_2 > 0} \tilde{H}^{\pm*}(\mathbf{r}, f) [\tilde{\Theta}_{ij}^{\pm}(\mathbf{r}, \mathbf{s}, f) + \tilde{\Theta}_{ji}^{\pm}(\mathbf{r}, \mathbf{s}, f)] \tilde{H}^{\pm}(\mathbf{s}, f) d\mathbf{r} d\mathbf{s} / 2$

$T_{ij}^{2\pm}$ represents element ij of the symmetric and antisymmetric response transfer function matrices for three-dimensional gust.

Notice that interchange of subscripts is accomplished in the integrand to reduce the summation to $i \leq j$.

Reverting to panel summation form, we replace $\tilde{\Theta}_{ij}^{\pm}(\mathbf{r}, \mathbf{s}, f)$ by $\Theta_{ijmn}^{\pm}(f)$, where panels m and n are located at \mathbf{r} and \mathbf{s} , respectively. Then equation (2.23) reduces to

$$\phi^{\pm} = \sum_{j=1}^3 \left\{ T_{jj}^{2\pm} \Phi_j + 2 \sum_{i=1}^{j-1} T_{ij}^{2\pm} [\Phi_i \Phi_j]^{1/2} \right\} \quad (2.24)$$

where $T_{ij}^{2\pm} = \sum_{n=1}^N \left\{ |H_n^{\pm}|^2 (\theta_{ijn}^{\pm} + \theta_{jin}^{\pm}) / 2 \right.$

$$\left. + \sum_{m=1}^N [\operatorname{Re}(H_m^{\pm*} H_n^{\pm}) \operatorname{Re}(\theta_{ijmn}^{\pm} + \theta_{jimn}^{\pm}) - \operatorname{Im}(H_m^{\pm*} H_n^{\pm}) \operatorname{Im}(\theta_{ijmn}^{\pm} + \theta_{jimn}^{\pm})] \right\}$$

in analogy with (2.18).

2.7 COUPLING BETWEEN GUST COMPONENTS

Only in the 3-D gust response formulation is the coupling between gust components fully represented. This is illustrated as follows. Let σ_j denote the RMS response amplitude due to gust component j , and let ρ_{ij} represent the correlation coefficient between responses due to gust components i and j . By definition, $|\rho_{ij}| \leq 1$, and the total mean square response amplitude, σ^2 , equals the integral of the response power spectrum; i. e.,

$$\sigma^2 = \int_0^{\infty} \phi(f) df \quad (2.25)$$

Substituting from equation (2.23), taking the square root, and applying the above definitions then yields

$$\sigma = (\sigma_1^2 + \sigma_2^2 + \sigma_3^2 + 2\sigma_1\sigma_2\rho_{12} + 2\sigma_2\sigma_3\rho_{23} + 2\sigma_3\sigma_1\rho_{31})^{1/2} \quad \text{3-D (2.26)}$$

where $\sigma_j^2 = \int_0^{\infty} [T_{jj}^{2+}(f) + T_{jj}^{2-}(f)] \Phi_j(f) df$

and $\rho_{ij} = \int_0^{\infty} [T_{ij}^{2+}(f) + T_{ij}^{2-}(f)] [\Phi_i(f)\Phi_j(f)]^{1/2} df / \sigma_1\sigma_2$

It can be shown that when the 3-D formulation is reduced to the conventional 2-D formulation by assuming that the vertical dimensions of the aircraft are negligible, only coupling between responses due to longitudinal and lateral gust components remains; i. e.,

$$\sigma = (\sigma_1^2 + \sigma_2^2 + \sigma_3^2 + 2\sigma_1\sigma_2\rho_{12})^{1/2} \quad \text{2-D (2.27)}$$

Moreover, even this coupling is irrelevant if response to longitudinal gust is not included in the aerodynamic model.

Finally, if the 3-D gust response formulation is reduced to the 1-D turbulence limit by assuming that the transverse (vertical and lateral) dimensions of the aircraft are small compared to those wavelengths which are present in the spatial distribution of gust velocity and which excite significant structural responses, then the power spectrum of the combined gust response equals the sum of the power spectra due to the individual gust components. The RMS amplitude of the total response then reduces to

$$\sigma = (\sigma_1^2 + \sigma_2^2 + \sigma_3^2)^{1/2} \quad \text{1-D} \quad (2.28)$$

2.8 CROSS TRANSFER FUNCTIONS

In dynamic response testing, it is common practice to install a gust probe on the aircraft for the purpose of obtaining time histories of one or more components of the gust velocity during flights through turbulence. Since the aircraft is also instrumented to obtain response time histories, statistical comparisons between outputs and inputs may be accomplished. These comparisons often assume two forms. In one case input and output power spectra are computed. These are related by transfer functions according to equation (2.23). In the other case, cross spectra between inputs and responses are computed, so that an analogous expression involving cross transfer functions is required (Reference 10).

Instead of correlating a response with itself, as we did in equation (A-2) of Appendix A, we could cross-correlate it with component i of the gust velocity measured by a probe located at point p . Straightforward application of the preceding methods

yields a corresponding cross spectrum, $\phi_i(f)$. By analogy with equation (2.22), define symmetric and antisymmetric probe coherence matrices

$$\tilde{\Lambda}_{ij}^{\pm}(\mathbf{p}, \mathbf{s}, f) = [\tilde{\Lambda}_{ij}(\mathbf{p}, \mathbf{s}, f) \pm \tilde{\Lambda}_{ij}(\mathbf{p}', \mathbf{s}, f)]/2 \quad (2.29)$$

where $\tilde{\Lambda}_{ij}(\mathbf{p}, \mathbf{s}, f) = \epsilon_i \Gamma_{ij}(\hat{\mathbf{s}} - \hat{\mathbf{p}}, f) n_j(s)$

and $\epsilon_1 = \epsilon_3 = 1$, $\epsilon_2 = p_2/|p_2|$

$\tilde{\Lambda}_{ij}(\mathbf{p}, \mathbf{s}, f)$ represents element ij of the probe coherence matrix, and equals the coherence between gust velocity component i measured at \mathbf{p} , and component j of the normalwash measured at \mathbf{s} , where both components are referenced in phase to the $x = 0$ plane. Then

$$\phi_i(f) = \phi_i^+(f) + \phi_i^-(f) \quad (2.30)$$

where $\phi_i^{\pm}(f) = e^{2\pi i f p_1/U} \sum_{j=1}^3 H_{ij}^{\pm}(f) [\Phi_i(f)\Phi_j(f)]^{1/2}$

and $H_{ij}^{\pm}(f) = \int_{s_2 > 0} \tilde{\Lambda}_{ij}^{\pm}(\mathbf{p}, \mathbf{s}, f) \tilde{H}^{\pm}(\mathbf{s}, f) d\mathbf{s}$

H_{ij}^{\pm} represents element ij of the cross transfer function matrices which relate to the symmetric (+) and antisymmetric (-) parts of gust component i measured at the probe, that portion of the response which is of corresponding symmetry, and which results from the specific action of gust component j upon the entire aircraft.

If we let $\mathbf{p}' \rightarrow \mathbf{p}$ in equation (2.29), then by virtue of (2.21), we obtain

$$\tilde{\Lambda}_{1j}^- = \tilde{\Lambda}_{2j}^+ = \tilde{\Lambda}_{3j}^- = 0 \quad (2.31)$$

Contrails

so that $\phi_1^-(f) = \phi_2^+(f) = \phi_3^-(f) = 0$. Therefore, when the gust probe is located in the plane of symmetry, the response cross spectra with respect to longitudinal and vertical gust velocity originate only from symmetric gust input, and the lateral cross spectrum originates only from antisymmetric input.

The panel summation equivalent of equation (2.30) is obtained by replacing $\tilde{\Lambda}_{ij}^\pm(\mathbf{p}, \mathbf{s}, f)$ by $\Lambda_{ij0n}^\pm(f)$, where 0 represents the probe location \mathbf{p} , and panel n is located at \mathbf{s} . Then

$$\phi_i^\pm = e^{2\pi i f p_1/U} \sum_{j=1}^3 H_{ij}^\pm [\Phi_i \Phi_j]^{1/2} \quad (2.32)$$

$$\text{where } H_{ij}^\pm = \sum_{n=1}^N \Lambda_{ij0n}^\pm H_n^\pm$$

SECTION III

AIRCRAFT DESCRIPTION

The frequency response functions for loads and deflections constitute from a design standpoint the essential dynamic response description of an aircraft. These are obtained by first solving the governing equation, which is most conveniently cast into matrix form, corresponding to the aerodynamic and structural representation of the aircraft as a finite number of discrete elements.

3.1 GOVERNING EQUATION

The dynamic response of an airplane flying through turbulence is described by the matrix equation of the balanced loads:

$$[M] \{ \ddot{X} \} + [K] \{ X \} = \{ L^X \} + \{ L^W \} \quad (3.1)$$

where $[M]$ = mass matrix

$[K]$ = stiffness matrix

$\{ X \}$ = incremental deflections (column matrix)

$\{ L^X \}$ = loads due to incremental deflections

$\{ L^W \}$ = gust loads

and the dot denotes a time derivative.

The time dependence of the loads and deflections may be taken as $e^{i\omega t}$, where ω is the excitation frequency. This entails no loss of generality, since the total response is eventually obtained by integrating over the range of excitation frequencies.) Then

$$\{ \ddot{X} \} = -\omega^2 \{ X \} \quad (3.2)$$

and it is possible to write

$$\{L^X\} = [D] \{X\} \quad (3.3)$$

where $[D]$ is a function of ω and incorporates all terms involving time derivatives of $\{X\}$. In analogy with equation (3.3) we may also write

$$\{L^W\} = [G] \{w\} \quad (3.4)$$

where $\{w\}$ contains the gust normalwash measured at the reference point of each aerodynamic surface panel.

3.2 MODAL ANALYSIS

The free vibration mode shapes which comprise the columns of the modal matrix $[\Phi]$ are determined by solving equation (3.1) in the absence of the loads $\{L^X\}$ and $\{L^W\}$. The result may be written

$$[K][\Phi] - [M][\Phi] [\bar{\omega}^2] = 0 \quad (3.5)$$

where the modal eigenfrequencies are contained in the diagonal matrix $[\bar{\omega}^2]$. The eigenfrequencies of the rigid body modes appear as zeros in the matrix. It is easily shown that the modes are orthogonal with respect to $[K]$ and $[M]$ so that

$$[\bar{K}] = [\bar{M}] [\bar{\omega}^2] \quad (3.6)$$

where $[\bar{K}] = [\Phi]^T [K] [\Phi]$

and $[\bar{M}] = [\Phi]^T [M] [\Phi]$

are the generalized stiffness and mass matrices, respectively, and the superscript T denotes the matrix transpose.

Since the modes form a mathematically complete set, $\{X\}$ may be expanded by linear superposition of mode shapes; i.e.,

$$\{X\} = [\Phi]\{q\} \quad (3.7)$$

The final step of the solution consists of determining the modal amplitudes $\{q\}$ which will satisfy equation (3.1) when $\{L^X\}$ and $\{L^W\}$ are reinserted.

Accordingly, by substituting equations (3.2), (3.3) and (3.7) into (3.1), multiplying by $[\Phi]^T$ and then applying equation (3.6) we obtain the modal or generalized form of equation (3.1):

$$[\bar{M}(\bar{\omega}^2 - \omega^2)]\{q\} = \{Q^X\} + \{Q^W\} \quad (3.8)$$

where $\{Q^X\} =$ generalized loads due to deflections = $[\bar{D}]\{q\}$

$\{Q^W\} =$ generalized gust loads = $[\Phi]^T[G]\{w\}$

and $[\bar{D}] = [\Phi]^T[D][\Phi]$

transposing $\{Q^X\}$ to the left hand side of the equation and solving for $\{q\}$ then yields

$$\{q\} = [B]^{-1} \{Q^W\} \quad (3.9)$$

where $[B] = [\bar{M}(\bar{\omega}^2 - \omega^2)] - [\bar{D}]$

and the superscript -1 denotes the matrix inverse.

3.3 DETAILED SOLUTION

The terms $\{L^X\}$ and $\{L^W\}$ in equation (3.1) must be examined

further to provide an explicit representation of structural damping, aerodynamic induction, and control system effects in equation (3.9).

Conventional practice assumes that the structural damping in the modes is proportional to and 90° out of phase with the generalized elastic loads $[\Phi]^T \{L_E\}$, where

$$\{L_E\} = [K] \{x\} \quad (3.10)$$

and the subscript E signifies elastic response. Then by virtue of equations (3.6) and (3.7), the generalized structural damping matrix may be written

$$i[g] [\Phi]^T \{L_E\} = i[\bar{M}\bar{\omega}^2 g] \quad (3.11)$$

where $[g]$ is a real matrix containing the structural damping coefficients for each mode.

Let $[A^X]$ and $[A^W]$ denote the aerodynamic induction matrices which relate aerodynamic loads to incremental deflections and gust normalwash, respectively.

Automatic control systems may respond to either gusts or deflections according to the sensors employed. Deflections in this case include elastic loads, since a direct dependence exists through equation (3.10). A sensor in the form of a differential pressure gust probe mounted on a boom would be sensitive to both gusts and deflections, for example. Accordingly, let $[S^X]$ and $[S^W]$ represent the matrices which relate aerodynamic loads resulting from control surface deflections, to incremental deflections and gust normalwash, respectively, as detected by sensors.

Contrails

Referring to equations (3.3) and (3.4) we may now deduce that

$$[\bar{D}] = i[\bar{M}\omega^2 g] + [\bar{A}^X] + [\bar{S}^X] \quad (3.12)$$

where $[\bar{S}^X] = [\Phi]^T [S^X] [\Phi]$

and $[\bar{A}^X] = [\Phi]^T [A^X] [\Phi]$

Similarly,

$$[G] = [A^W] + [S^W] \quad (3.13)$$

Substituting equations (3.12 and 3.13) into (3.8) enables us to write (3.9) as

$$\{q\} = [B]^{-1} \{Q^W\} \quad (3.14)$$

where $[B] = [\bar{M}(\omega^2(1 + ig) - \omega^2)] - [\bar{A}^X] - [\bar{S}^X]$

and $\{Q^W\} = [\Phi]^T \left([S^W] + [A^W] \right) \{w\}$

3.4 LOADS AND DEFLECTIONS

Elastic loads associated with design calculations will be indicated by affixing a prime, to distinguish them from the elastic loads we have so far considered. The associated stiffness matrix will also be primed, so that in analogy with equation (3.10),

$$\{L'_E\} = [K'] \{X\} \quad (3.15)$$

Substituting equation (3.7) into (3.15) and recognizing that only

the elastic modes contribute, we obtain

$$\{L'_E\} = [K'] [\Phi_E] \{q_E\} \quad (3.16)$$

Loads and deflections are computed by substituting into equations (3.16) and (3.7), respectively, the modal amplitudes obtained by (3.14). In practice, as many modes are used as is necessary to represent the structure over the range of excitation frequencies of interest. The upper limit of this range is dictated by the rapid fall-off of the gust input spectra at higher frequencies.

3.5 FREQUENCY RESPONSE FUNCTIONS

The frequency response function $H(r, f)$ introduced in Paragraph 2.1 represents the complex amplitude ratio between a given structural response and a simple harmonic normalwash occurring at point r . However, the concept of a frequency response function need not be restricted to excitations applied at a point, but may be extended to include other inputs such as generalized forces or modal deflections. Under the discrete element formulation, each such frequency response function may be arranged in the form of a single row of elements in an influence coefficient matrix. These matrices will be denoted by the generic symbol $[H]$ accompanied by two subscripts which identify, respectively, the type of response and the input to which it is being related. This notation allows us to conveniently summarize for later use the results contained in equations (3.7), (3.13), (3.14) and (3.16). Thus,

$$\{x\} = [H_{Xq}] \{q\} = [H_{Xw}] \{w\} \quad (3.17)$$

$$\text{where } [H_{Xq}] = [\Phi]$$
$$[H_{Xw}] = [H_{Xq}] [H_{qw}]$$

$$\text{and } [H_{qw}] = [B]^{-1} [\Phi]^T [G]$$

Similarly,

$$\{L'_E\} = [H_{Lq}] \{q_E\} = [H_{Lw}] \{w\} \quad (3.18)$$

$$\text{where } [H_{Lw}] = [H_{Lq}] [H_{qw}]$$

$$\text{and } [H_{Lq}] = [K'] [\Phi_E]$$

3.6 SYMMETRY CONSIDERATIONS

If the aircraft is bilaterally symmetric, it is both customary and expedient to compute the symmetric and antisymmetric responses separately, and then to combine them. This procedure is analogous to the treatment of the turbulence field in Section II, so that the matrices appearing in Section III may be associated with either symmetric or antisymmetric responses. Similarly, the symmetry of the response will be specified by affixing a (+) or (-) superscript to the matrix.

SECTION IV

THREE-DIMENSIONAL GUST RESPONSE

The essential statistical information required to compute the gust design parameters of an aircraft subject to stationary random inputs is contained in the cross spectral densities of the resulting responses. Procedures for obtaining the response cross spectra will be developed by employing the methods derived in Reference 9. The necessary ingredients consist of an aircraft description in the form of the frequency response functions derived in Section III, and a representation of the gust environment developed in Section II and based upon the fundamental cross spectral density tensor of the turbulence velocity field.

4.1 RESPONSE CROSS SPECTRA

In accordance with the structural symmetry considerations discussed in Paragraph 3.6, let $\{x^\pm\}$ represent a set of symmetric or antisymmetric deflections. The cross spectral density between two responses measured on the aircraft may be taken as the product of one of the response amplitudes with the complex conjugate of the other. Thus, a matrix containing the cross spectra between the deflections is generated by the expression

$$[\phi_{XX}^\pm] = \{x^{\pm*}\} \{x^\pm\}^T \quad (4.1)$$

where the asterisk indicates the complex conjugate. The matrix of total cross spectra is obtained by summing the symmetric and

antisymmetric cross spectra. Thus,

$$[\phi_{XX}] = [\phi_{XX}^+] + [\phi_{XX}^-] \quad (4.2)$$

The diagonal of the matrix contains the response power spectra, since it consists of cross spectra between identical responses. It may also be observed that the transpose of the matrix is equal to its complex conjugate. This constitutes the Hermitian property common to all cross spectral matrices, and implies that nearly half of the matrix is redundant, since every element on one side of the diagonal is the complex conjugate of its transpose element.

The response power spectra, which were discussed in Paragraphs 2.3, 2.4 and 2.6, are of primary importance. However, as shown here, the generation of response cross spectra requires little additional effort. The power spectra of other responses such as local stresses, which can be linearly related to the calculated responses, may be easily obtained from the calculated response cross spectra if the associated linear coefficients are available.

4.2 MODAL CROSS SPECTRA

Let $[\phi_{qq}^\pm]$ and $[\Psi_{ww}^\pm]$ denote the cross spectral matrices of the symmetric and antisymmetric modal deflections and normal-washes, respectively. Substituting from equation (3.17) into (4.1) yields

$$[\phi_{XX}^\pm] = [H_{Xq}^{*\pm}] [\phi_{qq}^\pm] [H_{Xq}^\pm]^T = [H_{Xw}^{*\pm}] [\Psi_{ww}^\pm] [H_{Xw}^\pm]^T \quad (4.3)$$

where $[\phi_{qq}^{\pm}] = \{q^{*\pm}\} \{q^{\pm}\}^T = [H_{qw}^{\pm*}] [\Psi_{ww}^{\pm}] [H_{qw}^{\pm}]^T$

and $[\Psi_{ww}^{\pm}] = \{w^{*\pm}\} \{w^{\pm}\}^T$

Notice that the specific portion of equation (4.3) which establishes the diagonal of $[\phi_{XX}^{\pm}]$ corresponds identically to (2.18). Similar expressions for the elastic load cross spectra may be written based upon equation (3.18). Thus,

$$[\phi_{LL}^{\pm}] = [H_{Lq}^{\pm*}] [\phi_{qq}^{\pm}] [H_{Lq}^{\pm}]^T = [H_{Lw}^{\pm*}] [\Psi_{ww}^{\pm}] [H_{Lw}^{\pm}]^T \quad (4.4)$$

The above equations contain two possible procedures for computing loads and deflections. Since the two methods will necessarily yield identical results, a choice may be made on the basis of computational efficiency. Thus, it is easily verified that if the number of responses to be analyzed is significantly greater than the number of included modes, then intermediate calculation of the modal cross spectrum matrix in equations (4.3) and (4.4) may be more economical than the direct application of the normal-wash cross spectra, particularly since $[H_{Xq}^{\pm}]$ and $[H_{Lq}^{\pm}]$ are independent of frequency.

4.3 NONDIMENSIONAL COHERENCE TENSOR

The coherence properties of the three-dimensional turbulence field are described by the gust velocity coherence tensor, Γ , which was introduced in Paragraph 2.5. Since the tensor is symmetric, it has six distinct components, in general. However, by virtue of the rotational transformation given by equation (2.21), all nine components of the tensor may be expressed in terms of

the four distinct components of $\bar{\Gamma}$ in the rotated coordinate frame. Furthermore, when expressed in the rotated system, the tensor reduces to a function of only two scalar variables: the transverse separation distance, q , and the frequency, f . The scale of turbulence, L , appears as an additional parameter in the tensor formulations derived from the Dryden and von Karman spectral models for isotropic turbulence. However, the dependence upon L can be eliminated by expressing the two variables in a dimensionless form consisting of the distance in scale lengths,

$$\eta = q/L \quad (4.5)$$

and the frequency in radians per scale length,

$$\kappa = 2\pi fL/U \quad (4.6)$$

The four distinct components of $\bar{\Gamma}$ may then be written in the nondimensional form,

$$\bar{\Gamma}_{ij}(q, f) = \bar{\Gamma}_{ij}(\eta L, \kappa U/2\pi L) = \psi_{ij}(\eta, \kappa) \quad (4.7)$$

The gust velocity power spectra, $\Phi_i(f)$, may also be written in nondimensional form by normalizing them to the mean square value, $\langle u_i^2 \rangle$, of the corresponding gust velocity component, and expressing them as functions of the dimensionless frequency. Thus,

$\varphi_i(\kappa) d\kappa = \Phi_i(f) df / \langle u_i^2 \rangle$, so that

$$\Phi_i(f) = (2\pi L \langle u_i^2 \rangle / U) \varphi_i(\kappa) \quad (4.8)$$

An expression for the four gust velocity cross spectrum tensor components appearing in equation (2.13) is obtained by substituting

(4.7) and (4.8) into (2.19).

$$\Phi_{ij}(\mathbf{r}, f) = (2\pi L \langle u_i^2 \rangle / U) \psi_{ij}(\eta, \kappa) [\varphi_i(\kappa) \varphi_j(\kappa)]^{1/2} \quad (4.9)$$

The analytical forms of the two distinct gust velocity power spectra and the four distinct coherence tensor components in the rotated system are derived in Reference 9 for both the Dryden and von Karman spectral models. They are presented below in nondimensional form.

Dryden Spectral Model:

Let $\mu = \eta(1+\kappa^2)^{1/2}$, and K_n denote the nth order modified Bessel function of the second kind. Then

$$\varphi_1(\kappa) = 2/\pi(1+\kappa^2), \quad \varphi_2(\kappa) = \varphi_3(\kappa) = (1+3\kappa^2)/\pi(1+\kappa^2)^2 \quad (4.10)$$

and

$$\begin{aligned} \psi_{11} &= \mu K_1(\mu) - \mu^2 K_0(\mu) / 2 \\ -i\psi_{21} &= \kappa \mu^2 K_1(\mu) / 2^{1/2} (1+3\kappa^2)^{1/2} \\ \psi_{33} &= \mu K_1(\mu) - \mu^2 K_0(\mu) / (1+3\kappa^2) \\ \psi_{22} - \psi_{33} &= \mu^2 K_0(\mu) (1+\kappa^2) / (1+3\kappa^2) \end{aligned} \quad (4.11)$$

von Karman Spectral Model:

In the von Karman case, it is convenient to introduce a modified scale of turbulence, $\bar{L} = L\Gamma(1/3)/\Gamma(1/2)\Gamma(5/6) \simeq 1.339L$, and to define the corresponding $\bar{\kappa}$ and $\bar{\mu}$. Then

$$\varphi_1(\kappa) = 2/\pi(1+\kappa^2)^{5/6}, \quad \varphi_2(\kappa) = \varphi_3(\kappa) = (1+8\kappa^2/3)/\pi(1+\kappa^2)^{11/6} \quad (4.12)$$

Contrails

$$\begin{aligned} \text{and} \quad \psi_{11} &= B [\bar{\mu}^{5/6} K_{5/6}(\bar{\mu}) - \bar{\mu}^{11/6} K_{1/6}(\bar{\mu}) / 2] \\ -i\psi_{21} &= B \bar{\kappa} \bar{\mu}^{11/6} K_{5/6}(\bar{\mu}) / 2^{1/2} (1+8\bar{\kappa}^2/3)^{1/2} \\ \psi_{33} &= B [\bar{\mu}^{5/6} K_{5/6}(\bar{\mu}) - \bar{\mu}^{11/6} K_{1/6}(\bar{\mu}) / (1+8\bar{\kappa}^2/3)] \\ \psi_{22} - \psi_{33} &= B \bar{\mu}^{11/6} K_{1/6}(\bar{\mu}) (1+\bar{\kappa}^2) / (1+8\bar{\kappa}^2/3) \end{aligned} \tag{4.13}$$

where $B = 2^{1/6} / \Gamma(5/6) \simeq 0.9944$.

The gust velocity power spectra and coherence tensor components given by equations (4.10)-(4.13) are plotted in Figures 8-17. Notice that all four coherence tensor components are real except ψ_{12} , which is imaginary. This indicates that a $\pi/2$ phase difference exists between the coherent portions of the longitudinal and lateral gust components. Similarly, ψ_{33} exhibits a small negative value at low frequencies and large separation distances. Therefore, coherent vertical gust components have a phase difference of π under these conditions. It may be recalled that introducing a longitudinal separation merely imposes a further difference in phase, and has no effect upon the modulus of the coherence.

The one-dimensional turbulence field is characterized by complete coherence between like Cartesian gust components and complete incoherence between unlike components, regardless of frequency or separation distance. This corresponds to equating ψ_{ij} to unity if $i = j$, or zero if $i \neq j$. One-dimensional turbulence is approached in the 3-D case by letting $\kappa \rightarrow 0$ and $\eta \rightarrow 0$. This corresponds to low frequency and small separation distance. One may observe that the 1-D turbulence condition is approached in Figures 9-12 and 14-17 by advancing toward the lower left hand corner of each coherence plot.

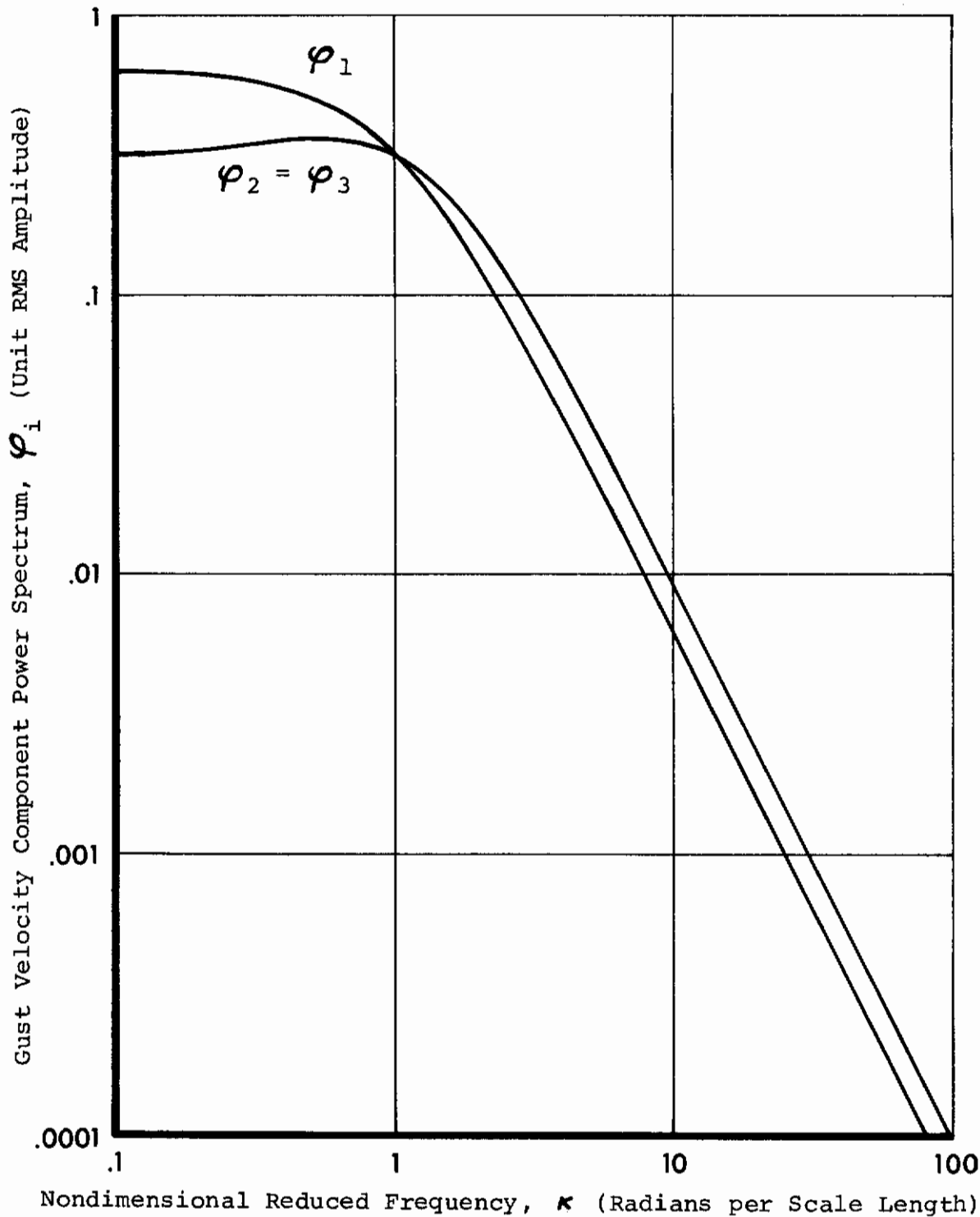


Figure 8. Power Spectra of Longitudinal and Transverse Gust Velocity Components Plotted vs. Reduced Frequency for the Dryden Case

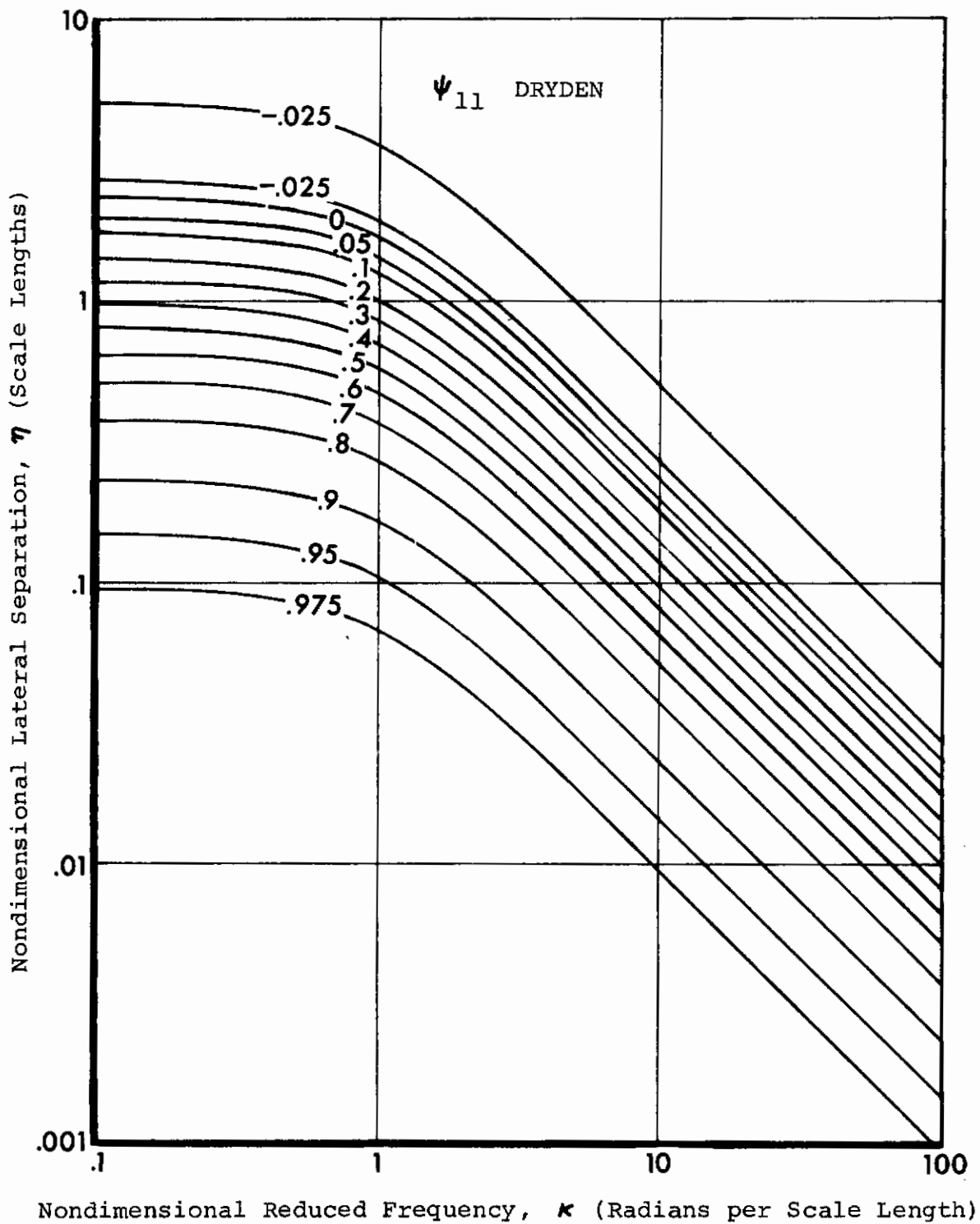


Figure 9. Coherence between Longitudinal Gust Components Plotted vs. Lateral Separation and Reduced Frequency for the Dryden Case

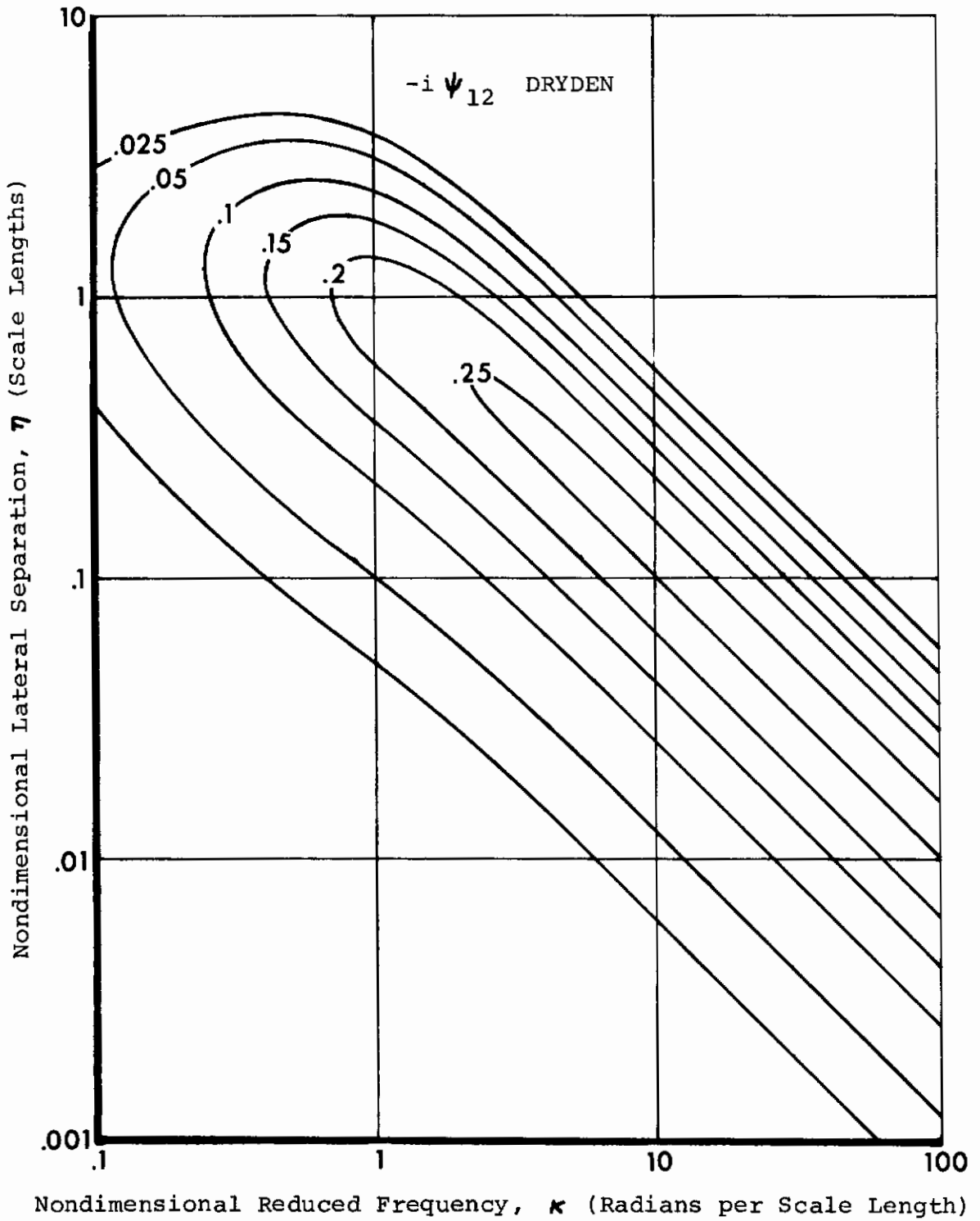


Figure 10. Imaginary Part of Coherence between Longitudinal and Lateral Gust Components Plotted vs. Lateral Separation and Reduced Frequency for the Dryden Case

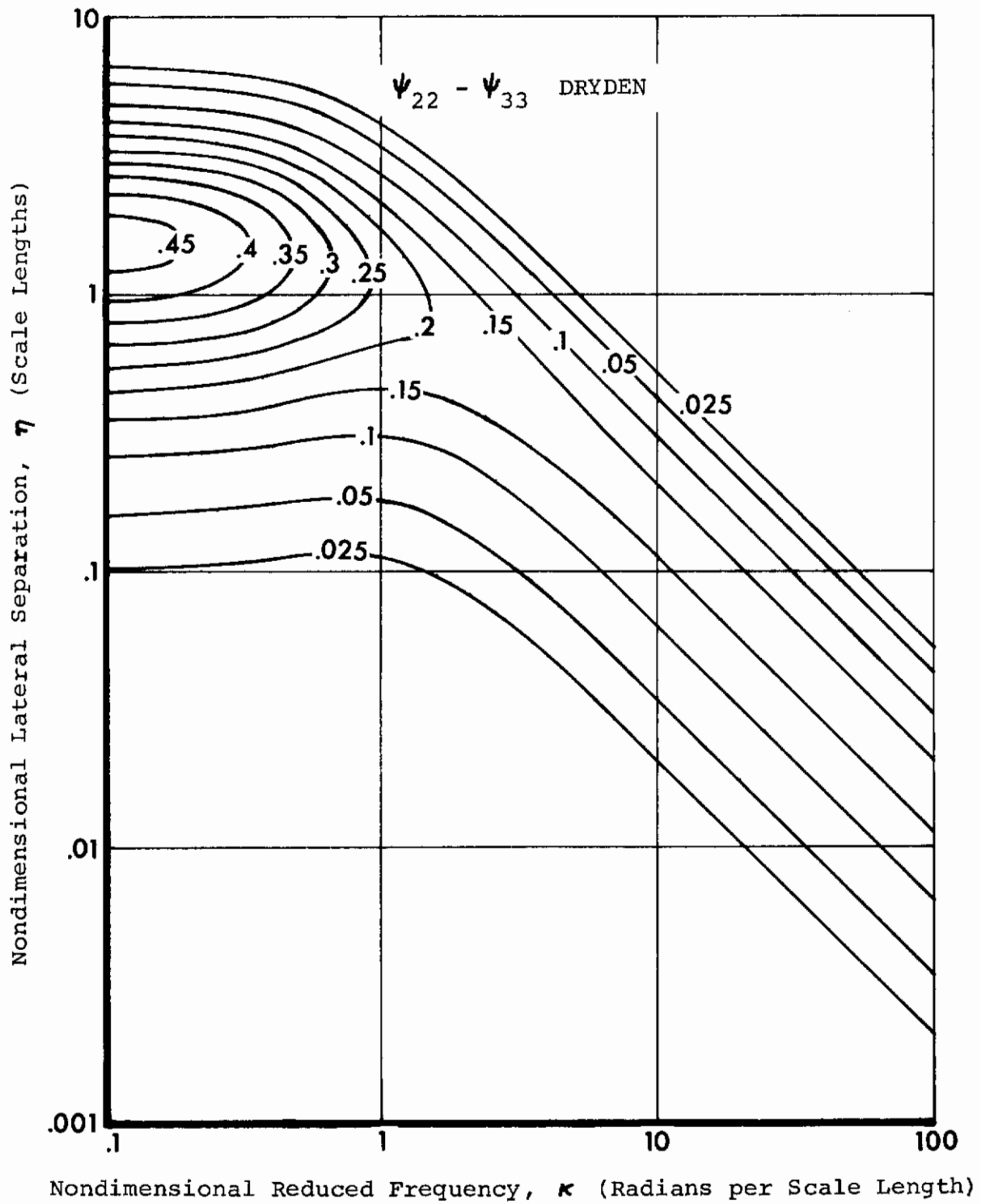


Figure 11. Excess of Coherence between Lateral Gust Components over Vertical Plotted vs. Lateral Separation and Reduced Frequency for the Dryden Case

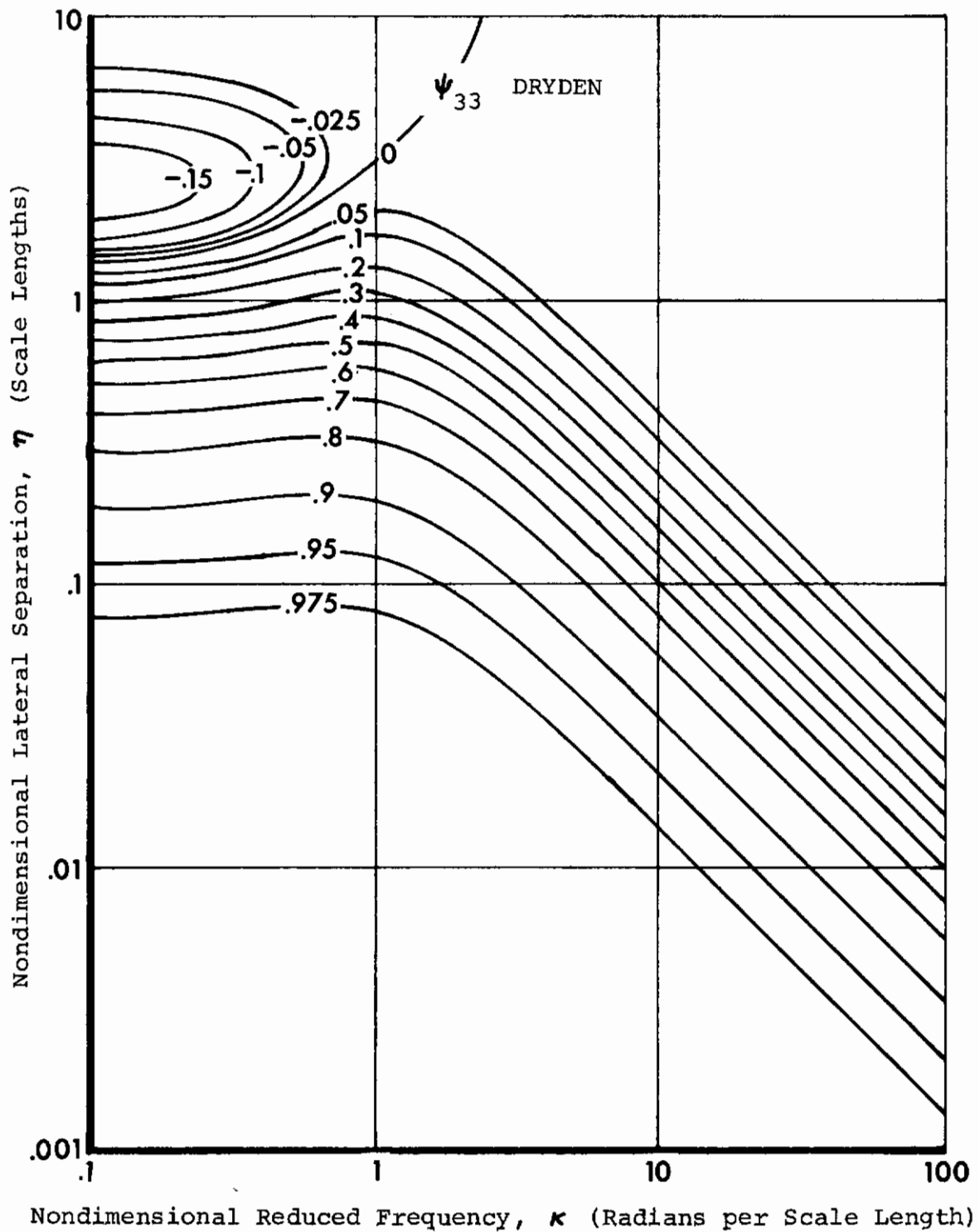


Figure 12. Coherence between Vertical Gust Components Plotted vs. Lateral Separation and Reduced Frequency for the Dryden Case

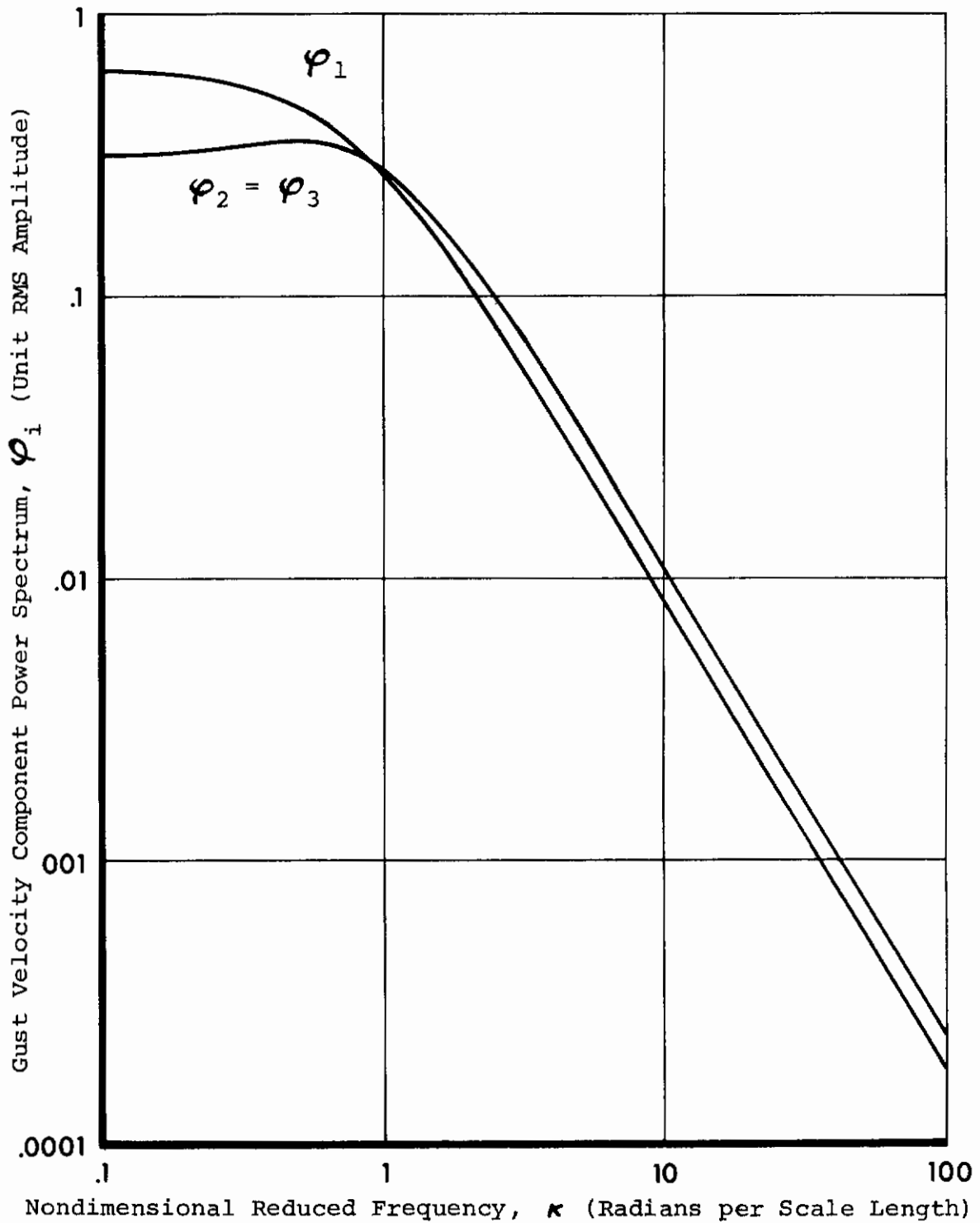


Figure 13. Power Spectra of Longitudinal and Transverse Gust Velocity Components Plotted vs. Reduced Frequency for the von Karman Case

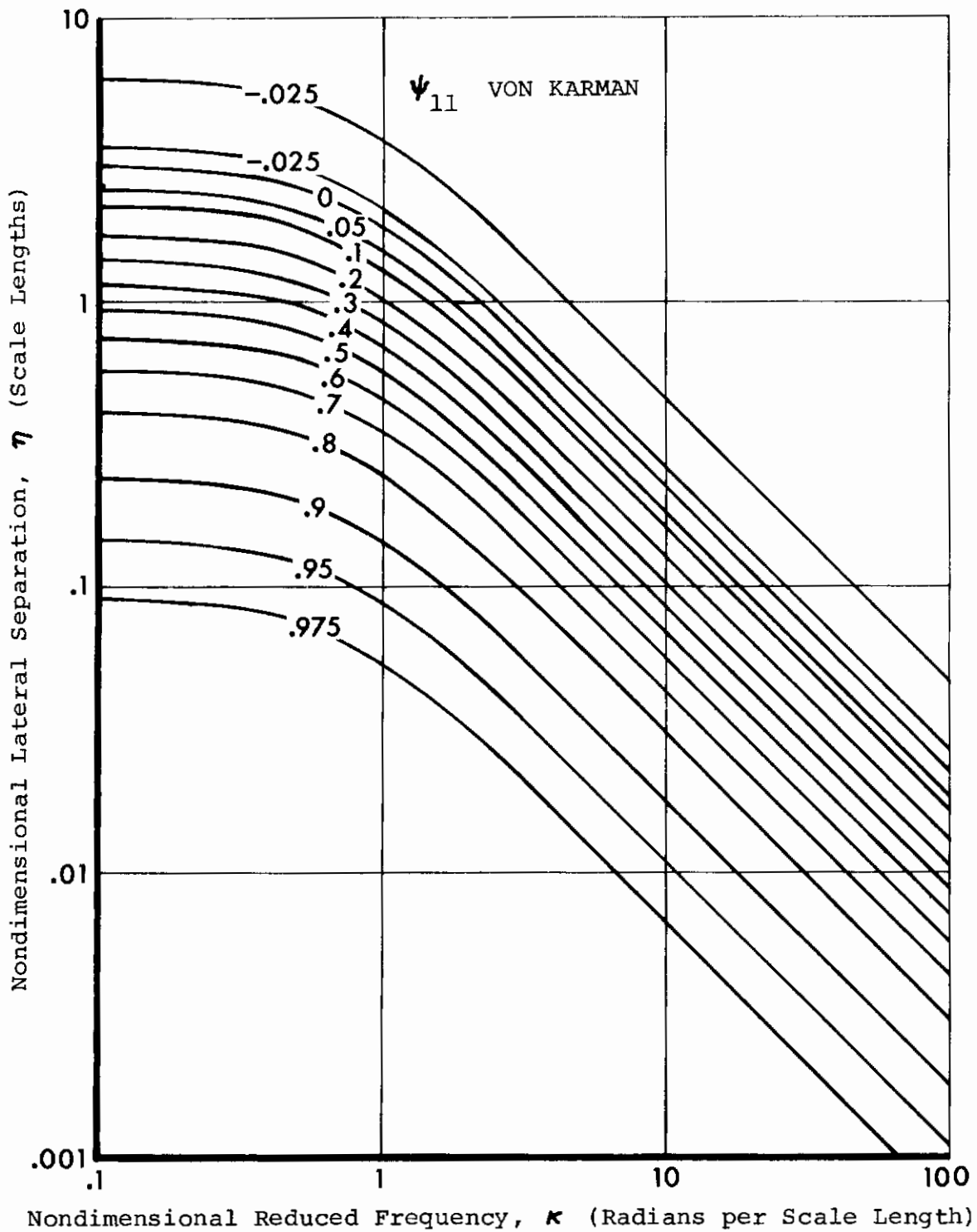


Figure 14. Coherence between Longitudinal Gust Components
Plotted vs. Lateral Separation and Reduced
Frequency for the von Karman Case

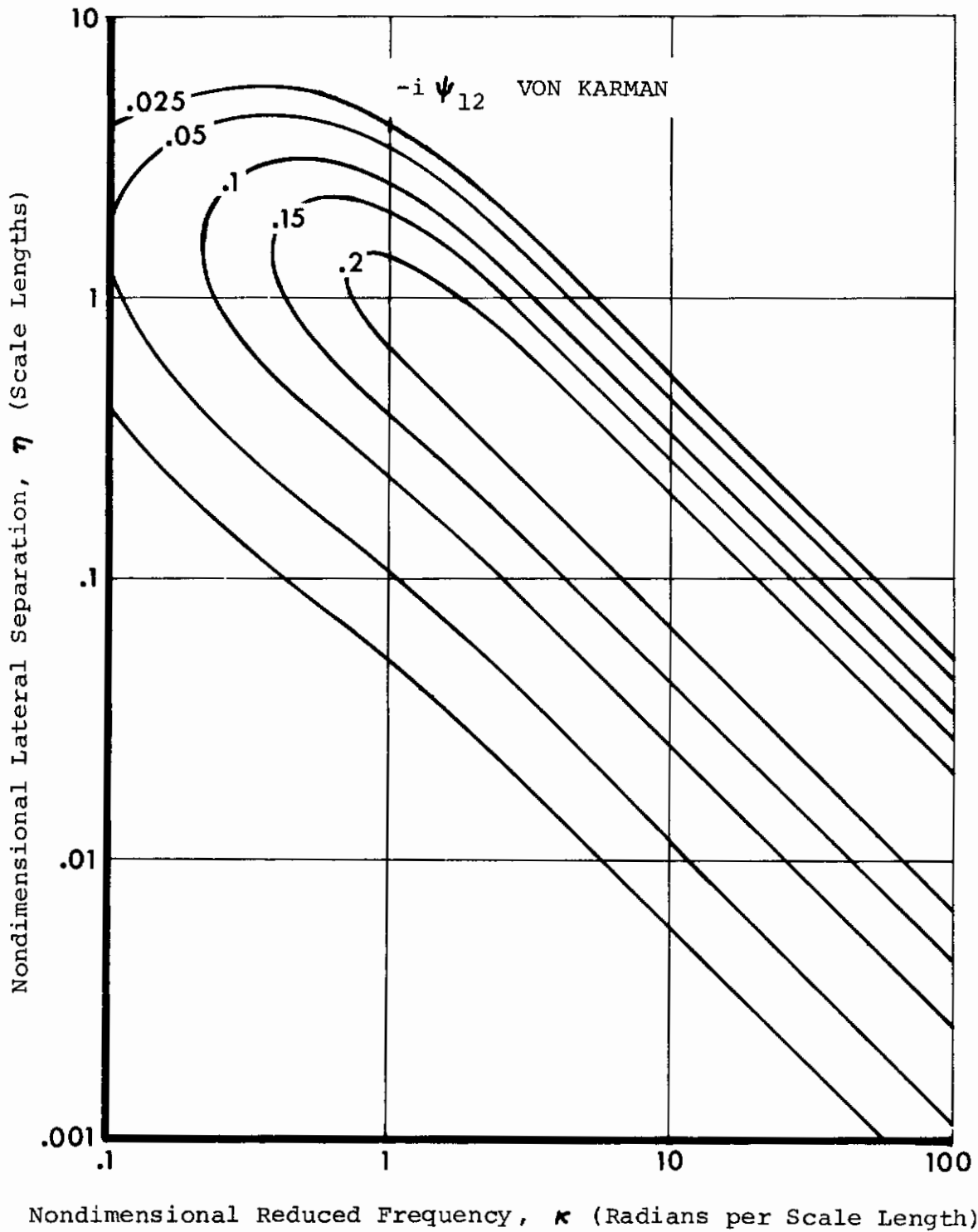


Figure 15. Imaginary Part of Coherence between Longitudinal and Lateral Gust Components Plotted vs. Lateral Separation and Reduced Frequency for the von Karman Case

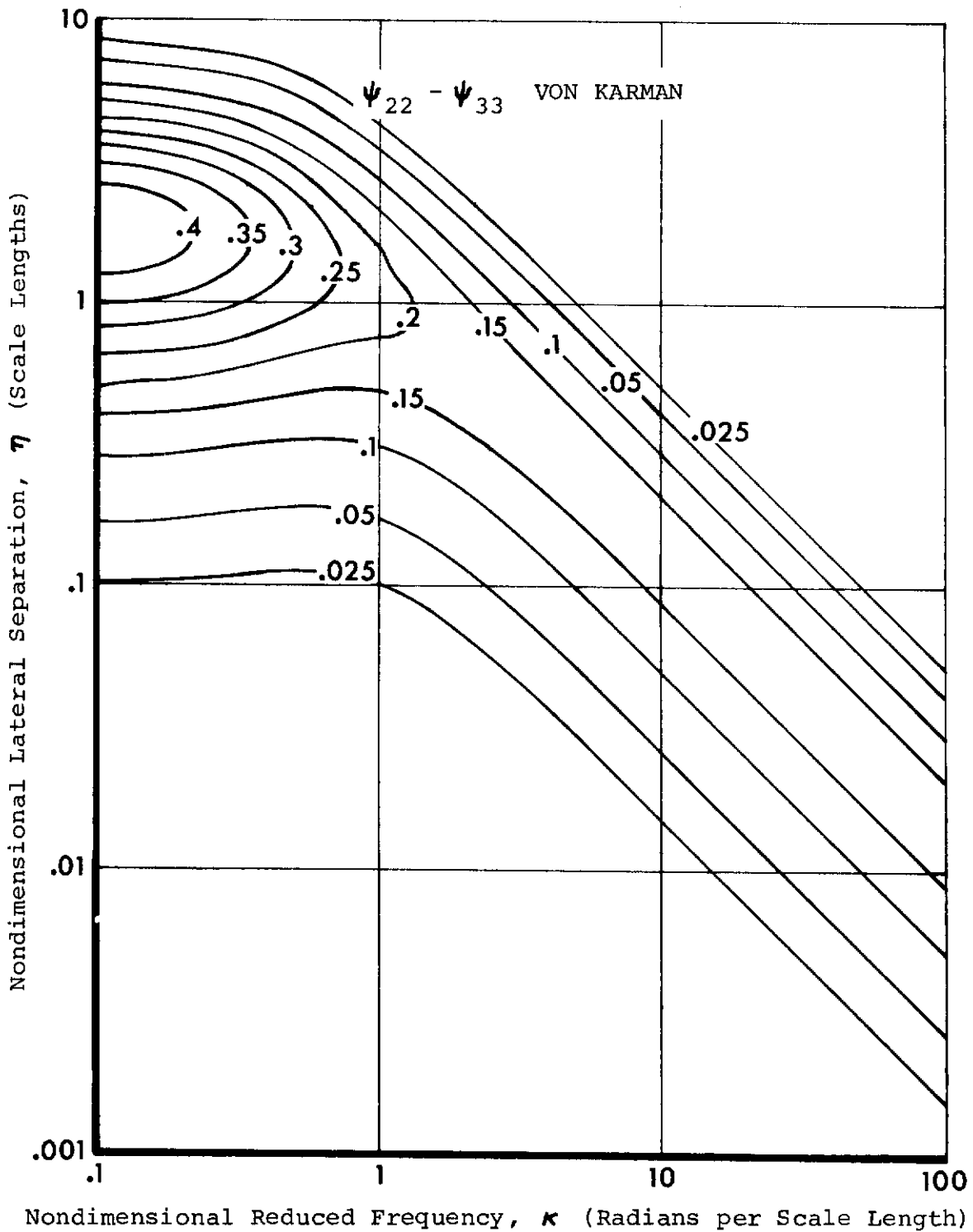


Figure 16. Excess of Coherence between Lateral Gust Components over Vertical Plotted vs. Lateral Separation and Reduced Frequency for the von Karman Case

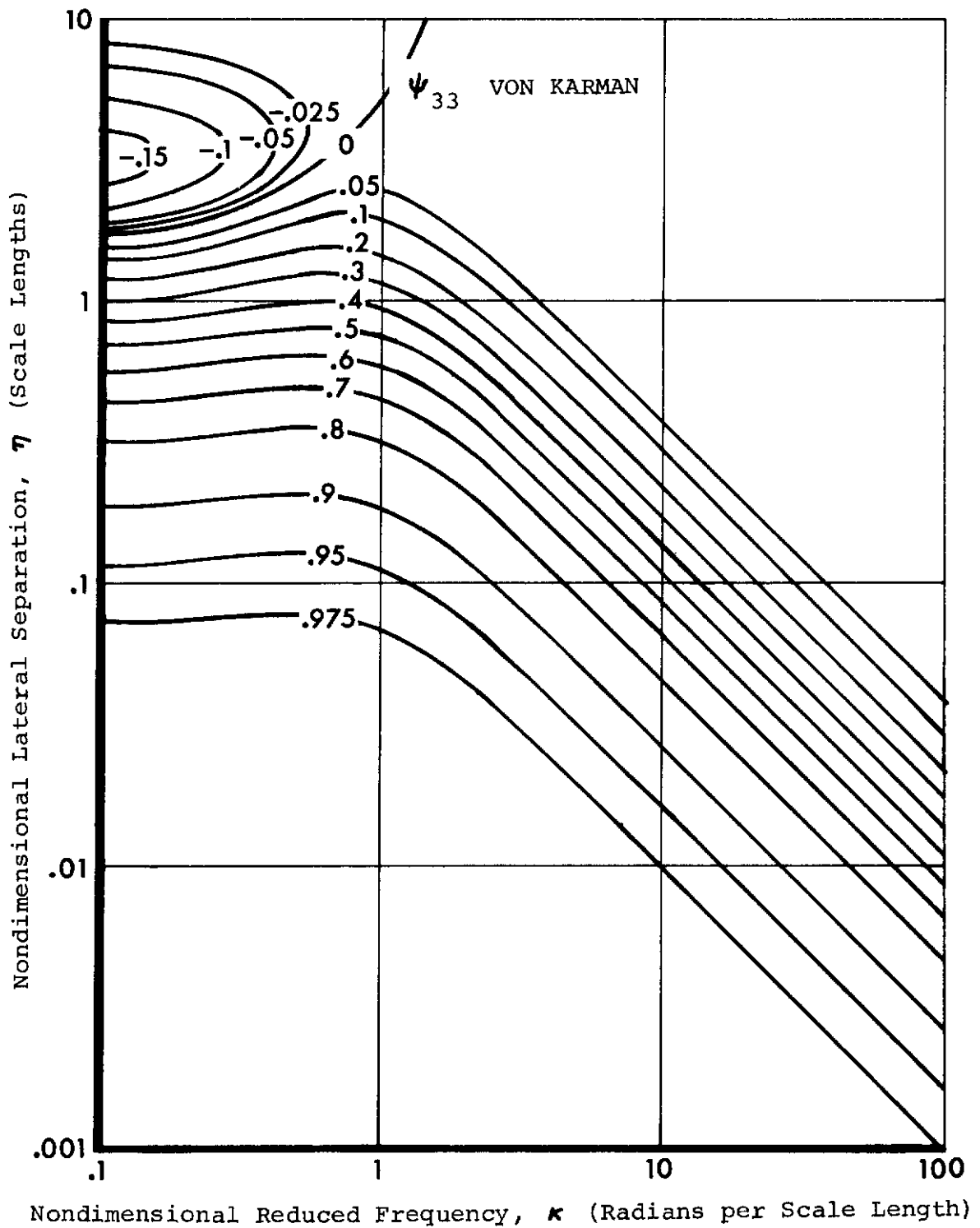


Figure 17. Coherence between Vertical Gust Components Plotted vs. Lateral Separation and Reduced Frequency for the von Karman Case

Contrails

For dynamic response applications, the coherence tensor components given by equations (4.11) or (4.13) may be stored in compact tabular form for rapid digital computation of the gust velocity cross spectra according to (4.9).

Examination of Figures 8-17 shows that although the Dryden and von Karman power spectra differ significantly, the contour plots of the corresponding coherence tensor components are almost indistinguishable. Evidently, the coherence properties of the turbulence field are relatively insensitive to the specific spectral distribution of gust velocities. This suggests the use of a single representative set of tensor components in all three-dimensional gust response calculations, including those in which flight-measured gust input spectra are utilized. Recent atmospheric measurements (Reference 11) have tended to yield power spectra which agree with the von Karman form, indicating that the tensor components given by equation (4.13) would be most appropriate for this purpose. The usual problem of estimating the scale of turbulence from flight-measured spectra is obviated inasmuch as dynamic response calculations are typically confined to the asymptotic range ($\eta < 1 < \kappa$), where uncertainty in L merely shifts the point (η, κ) approximately along a contour line, thus having little effect upon the value of the tensor component. This advantage may be utilized even more directly by replacing the tensor components by their appropriate asymptotic forms, which can be easily derived in the limit as L becomes large, and which depend only upon q/λ , where $\lambda = U/f$, the gust wavelength. This result, which may be termed the inertial range approximation, eliminates the need to

specify L in evaluating the coherence tensor components.

Unless the transverse dimensions of the aircraft are small compared to the scale of turbulence, three-dimensional effects will prevail even at the lowest frequencies. This conclusion may be established by reducing equations (4.11) and (4.13) to the low frequency limit, and is suggested by reference to the low frequency range ($\kappa < 1$) in Figures 9-12 and 14-17.

4.4 COMPUTATIONAL PROCEDURES

The aircraft description required for a response analysis consists of the frequency response functions, $H_n^\pm(f)$, defined by equation (2.16). These functions are generated for panel pairs $n = 1, \dots, N$, and for each of the required loads and deflections, according to matrix equations (3.17) and (3.18), respectively. If the number of responses to be calculated is much greater than the number of vibration modes employed, then it is most efficient to leave the frequency response functions factored into two matrices, which relate the desired responses to the modal amplitudes, and the modal amplitudes to the gust normalwashes, respectively, as shown.

The turbulence description for computing response power spectra consists of the gust normalwash cross spectra, $\Psi_{mn}^\pm(f)$, defined by equations (2.13), (2.14) and (2.17). Tables of the coherence tensor components given by equation (4.13) are entered with the nondimensional parameters defined by (4.5) and (4.6). The values extracted from the tables are then substituted into equation (4.9) to obtain the gust velocity cross spectrum tensor components required to evaluate the gust normalwash cross spectra.

The response power spectra are obtained by substituting $H_n^\pm(f)$ and $\psi_{mn}^\pm(f)$ into the matrix equivalent of equation (2.18), which is represented by (4.3) for deflections, and (4.4) for loads. The method involving intermediate calculation of the modal cross spectrum matrix, as explained in Paragraph 4.2, is used if the $H_n^\pm(f)$ is in the factored form described above.

If one wishes to utilize flight-measured gust spectra instead of the analytical spectra defined by equation (4.12), then equation (2.18) may be replaced by (2.24), which may be modified for greater efficiency by allowing the summation over gust components to be performed before the summation over panel pairs.

The turbulence description required for computing response cross spectra consists of the probe coherence matrix, $\Lambda_{ij0n}^\pm(f)$, obtained from equations (2.21), (2.24) and (4.7). The response cross spectra are computed by substituting $H_n^\pm(f)$ and $\Lambda_{ij0n}^\pm(f)$ into equation (2.32). This is a short calculation, since only a single summation is performed.

The RMS load amplitude, σ , and zero crossing rate, N_0 , are required in fatigue design calculations and are obtained from the response power spectrum. Thus,

$$\sigma = \left[\int_0^\infty \phi(f) df \right]^{1/2} \quad (4.14)$$

$$N_0 = \int_0^\infty \phi(f) f^2 df / \sigma \quad (4.15)$$

An aircraft may be instrumented to measure simultaneous time histories of gust components and structural responses during turbulence encounters, as described in Paragraph 2.8. This provides an opportunity to substantiate the analytical dynamic response

model of the aircraft by comparing the conventional frequency-dependent functions obtained from spectral analysis of the flight data, with the equivalent functions computed from the analytical model using the measured gust input spectra and applying the same flight parameters. Such an analysis typically includes the flight-measured transfer function, $T_i(f)$, cross transfer function, $H_i(f)$, and coherence function, $\gamma_i^2(f)$, which are defined as follows.

$$T_i(f) = [\phi(f)/\Phi_i(f)]^{1/2} \quad (4.16)$$

$$H_i(f) = \phi_i(f)/\Phi_i(f) \quad (4.17)$$

$$\gamma_i^2(f) = |\phi_i(f)|^2/\phi(f)\Phi_i(f) \quad (4.18)$$

Aerodynamic response to longitudinal gust is typically ignored in conventional analytical models used in gust response analysis. If this procedure is followed in the case of 3-D turbulence, then the coherence tensor components ψ_{11} and ψ_{12} associated with longitudinal gust are no longer required. Although this is likely to have little effect on the overall length of the calculation, it results in a considerable simplification of the equations used in the analysis, since all terms associated with the longitudinal gust component are omitted.

4.5 ONE-DIMENSIONAL TURBULENCE LIMIT

It may be recalled that the gust reference direction is taken normal to the aerodynamic input panel in defining the frequency response functions, $H_n^\pm(f)$. The frequency response functions generated for a conventional one-dimensional gust response

calculations are identical, except that an upwash is associated with symmetric response, and a sidewash with antisymmetric response, in keeping with the result shown in Figure 5. Furthermore, if the 1-D analytical model allows response to longitudinal gust, then a set of symmetric frequency response functions associated with backwash is also required. The 1-D frequency response functions are then summed over input panels to obtain a single cross transfer function, $H_i(f)$, for each gust component i .

Reference 9 shows that in the one-dimensional turbulence limit, fifteen of the eighteen elements vanish in the 3-D cross transfer function matrices, $H_{ij}^\pm(f)$, defined in equation (2.32). The three remaining elements reduce identically to the corresponding 1-D cross transfer functions described above; i.e.,

$$H_{11}^+(f) = H_1(f), H_{22}^-(f) = H_2(f), H_{33}^+(f) = H_3(f) \quad (1-D) \quad (4.19)$$

The squared transfer function matrix defined in equation (2.24) reduces in a similar fashion, except that

$$T_{11}^{2+}(f) = |H_1(f)|^2, T_{22}^{2-}(f) = |H_2(f)|^2, T_{33}^+(f) = |H_3(f)|^2 \quad (1-D) \quad (4.20)$$

The response power spectrum then reduces to

$$\phi(f) = \sum_{i=1}^3 |H_i(f)|^2 \Phi_i(f) \quad (1-D) \quad (4.21)$$

This may be compared with the 3-D case given by equation (2.24). Similarly, the response cross spectrum given by equation (2.32) becomes

$$\phi_i(f) = H_i(f) \Phi_i(f) \quad (1-D) \quad (4.22)$$

4.6 IMPROVEMENTS IN AIRCRAFT DESIGN AND ANALYSIS

The converse of the one-dimensional turbulence limit discussed in Paragraph 4.5 corresponds to large η and κ , which represent separation distance and reduced frequency, respectively. According to equations (4.5) and (4.6), $\eta = q/L$ and $\kappa = 2\pi fL/U$. Therefore, one may conclude that three-dimensional turbulence effects are important under the following conditions:

- o for aircraft of large transverse dimensions, q ,
- o in turbulence of small scale length, L , corresponding to low altitudes,
- o for high structural response frequencies, f ,
- o at low airspeeds, U .

Furthermore, it is obvious from geometrical considerations that ψ_{33} is the most significant coherence tensor component in three-dimensional gust response, since it represents the coherence between laterally separated vertical gust components. Therefore, the magnitude of 3-D gust response effects under given conditions may be assessed by entering the contour plot of Figure 17 with the corresponding values of η and κ to obtain ψ_{33} . If the resulting value of the correlation tensor component proves to be appreciably less than unity, then 3-D gust response effects may be assumed to prevail.

It may be stated in summary, that the three-dimensional gust response procedure, as outlined here, is mathematically identical

Contrails

to the conventional one-dimensional method except for the following two modifications, which do nothing more than account for the transverse coherence properties of the 3-D turbulence field:

- o The gust reference direction is taken normal to each aerodynamic input panel in the 3-D case, thereby resulting in only two sets of frequency response functions, one symmetric and the other antisymmetric.

The conventional 1-D procedure is identical, except that the gust reference direction is taken in the longitudinal and vertical directions in the symmetric case and in the lateral direction in the antisymmetric case. This results in three sets of frequency response functions if all three gust components are used.

- o Symmetric and antisymmetric normalwash cross spectra between input panels are calculated in the 3-D case in accordance with the isotropic turbulence model upon which the gust input spectra used in the 1-D case are based. This accounts for the transverse coherence properties of the 3-D turbulence field. The normalwash cross spectra and the frequency response functions are then substituted into the quadratic form represented by equation (2.18) to obtain the power spectra for symmetric and antisymmetric response.

In the 1-D analysis, each set of frequency response functions is merely summed over input panels as described

Contrails

in Paragraph 4.5. Products of the squared modulus of each sum and the corresponding gust input spectrum are then added together to obtain the response power spectrum as shown in equation (4.21).

Two-dimensional gust response analysis, which was mentioned briefly in Section I and Paragraph 2.2, will not be treated in any detail here, since the 3-D gust response analysis reduces identically to the 2-D case when the vertical dimensions of the aircraft become negligible. Furthermore, because lateral gust becomes uncoupled, the 2-D calculation as usually performed is actually longer than the 3-D. This follows from the fact that lateral gust response is treated separately, and the quadratic form that accounts for coherence between the remaining gust components is not reduced in size.

Three-dimensional gust response analysis provides a single set of load amplitudes and zero crossing rates for use in fatigue design, since coupling between gust components is accounted for in a mathematically rigorous manner, as described in Paragraph 2.7. Fatigue damage due to vertical and lateral gusts is often artificially separated in the 1-D analysis. The conventional 2-D analysis is subject to the same limitation, even though it accounts for coherence between the remaining gust components.

The functions which are obtained by spectral analysis of flight-test data, as described in Paragraph 4.4, are particularly sensitive to the transverse coherence properties of the turbulence field. Consequently, for aircraft of large transverse dimensions, the discrepancy between test results and the parallel 1-D analysis

may hinder efforts to substantiate the analytical model. This problem is avoided by employing the 3-D gust response analysis. In fact, as explained in Paragraphs 5.2 and 5.3, the coherence properties of the turbulence field may provide a means for validating the induction characteristics of the aerodynamic model.

SECTION V

OUTLINE OF RECOMMENDED RESEARCH

Current gust design criteria specifications implicitly assume that the atmospheric turbulence environment is three-dimensional, and that it is isotropic in its coherence properties. For example: (1) the power spectra of the gust velocities used as input to our analytical models are derived from isotropic turbulence theory, (2) gust criteria specifications used in aircraft design calculations typically assume that the vertical and lateral scales of turbulence are equal, although RMS values may be allowed to differ at low altitudes, and (3) in deriving these criteria from aircraft response records, a spanwise averaging correction is often applied to account for three-dimensional turbulence.

Only in the gust response calculation itself are these assumptions customarily ignored. There the turbulence field is generally taken to be one-dimensional, and the responses to vertical and lateral gusts are separated. However, the assumption of a three-dimensional turbulence environment is compatible with existing criteria and design procedures. Moreover, no significant increase in computational effort would be required to account for three-dimensional turbulence in gust response calculations. As explained in Paragraph 4.4, the calculation may be reduced to easily manageable size by use of the three-dimensional gust response method introduced in Section II.

The research plan outlined here is designed to achieve four interrelated objectives: (1) implementation of three-dimensional

gust response computational methods, (2) validation of these methods by comparison with dynamic response test results, (3) incorporation of these methods into current design procedures, (4) development of new methods and applications, including treatment of aircraft response to turbulence conditions which depart from current ideal assumptions.

5.1 IMPLEMENTATION OF COMPUTATIONAL METHODS

It is recommended that an efficient dynamic response computer program be developed to calculate aircraft loads and deflections resulting from three-dimensional turbulence. The program should furnish response power spectra, as well as RMS amplitude ratios and zero crossing rates used in fatigue design calculations. The program should also be capable of furnishing the various statistical functions of frequency that correspond directly with those obtainable from dynamic response test of an aircraft employing a gust probe. These include flight-measured transfer functions, cross transfer functions and coherence functions. The program should be capable of accepting flight-measured gust velocity power spectra as input for comparison with flight results, as well as being able to generate the Dryden and von Karman analytical spectra for use when the RMS gust velocity and scale of turbulence are furnished. The gust velocity coherence tensor used in the calculation should be computed from stored tables according to both the Dryden and von Karman turbulence models, so that comparisons can be made. An option should be provided to compute the exact analytical coherence tensor when the scale of turbulence is furnished,

or to utilize the inertial range approximation when it is not. The inertial range approximation was discussed in Paragraph 4.3.

The computer program would utilize the aircraft response model developed in Section III, so that automatic control systems could be included, and the number of vibration modes could be easily adjusted. Modern, efficient eigenvalue methods such as the QR transformation would be utilized to compute the vibration modes, so that the number of modes included would have little effect upon the speed of the computation. An option would be available to compute loads and deflections directly from the normalwash cross spectra, or to compute the modal cross spectra first, if a large number of responses are involved. Both methods are contained in equations (4.3) and (4.4). RMS amplitudes and zero crossing rates for use in fatigue design would also be furnished by the program.

Doublet lattice methods would be applied to obtain three-dimensional aerodynamic influence coefficients, and the new subsonic kernel function formulation developed in Appendix B would be employed to reduce computational effort by the use of tabular interpolation. An option would be provided to reduce the aerodynamic influence coefficient matrices to a diagonal form which is effectively equivalent to modified strip theory. This would make it possible to establish the effects of the aerodynamic model on the three-dimensional gust response calculation, as mentioned in Section IV.

An optional breakdown would be provided showing the relative portions of the calculated response quantities attributable to the

various categories of gust input; i.e., vertical, lateral, coupled, symmetric and antisymmetric. Options to reduce the turbulence model to one and two dimensions would also be included so that effects of dimensionality could be examined.

The computer program would be applied to analyze the gust response of an existing aircraft for which pronounced three-dimensional turbulence effects and combined vertical and lateral gust responses could be expected. An airplane having a T-tail, wing pylons and a large wing span would be ideal for this purpose. Preferably, the analysis would be performed so that a direct comparison between corresponding analytical and flight test results could be conducted as described in Paragraph 5.2.

5.2 VALIDATION BY FLIGHT TEST COMPARISON

Figure 18 outlines the sequence of calculations required to compare results obtained from the analytical model with data derived from dynamic response flight test measurements. The operations involved in processing the flight test data are indicated on the left hand side of the diagram, while the remainder of the diagram shows the computational sequence followed to obtain corresponding data from the analytical gust response model. The computer program which incorporates the analytical model is described in Paragraph 5.1.

The aircraft is assumed to be instrumented so that time histories of gust velocity components as well as response quantities such as loads and accelerations can be measured during flights through turbulence. The figure indicates that the digitized time

Contrails

histories of the gust velocity components measured by the gust probe are corrected for aircraft motion by gust reduction. The measured time histories are then spectral analyzed to obtain the power spectra of both the responses and the gust components. Cross spectra between responses and gust components are also calculated.

Corresponding response power spectra and cross spectra are generated by the analytical model program as described in Section IV, using as input the gust power spectra obtained from the test data, and assuming the average conditions which existed during the test flight. Transfer functions, cross transfer functions and coherence functions are then calculated from the power spectra and cross spectra generated from the analytical model. These functions are also calculated from the power spectra and cross spectra obtained from the flight test so that comparisons can be made as indicated in the figure.

A comparison between flight test measured and theoretical gust responses for an analytical model employing one-dimensional turbulence is given in Reference 10. The possibilities for substantiation of analytical results are appreciably enhanced when the three-dimensional turbulence model is used, since the statistical coherence properties of the turbulence field are thereby preserved. Cross spectra between responses and gust inputs are particularly sensitive to the coherence of the turbulence field which exists within the spatial bounds of the aircraft. Consequently, cross transfer functions and coherence functions, both of which depend upon the cross spectra, are expected to show better agreement between test and analysis in the 3-D case.

Contrails

Because of the coherency augmentation effect of aerodynamic induction discussed in Paragraph 5.3, it is also expected that cross spectral results will be quite sensitive to the aerodynamic representation. Transfer functions and coherence functions derived from three-dimensional gust response analysis will therefore constitute unique diagnostic tools for assessing the aerodynamic portion of the analytical model.

Data derived from power spectra, such as RMS responses and zero crossing rates, are expected to show improved spanwise distributions, often accompanied by a general reduction due to spanwise averaging of the gust input.

It is recommended that the test flight chosen for comparison be approximately five minutes in duration to provide sufficient statistical stability. An RMS gust velocity of three feet per second with reasonable stationarity should be the minimum criterion for acceptance so that extraneous inputs and gust reduction errors will represent a sufficiently small proportion of the final measurement.

If the test aircraft is instrumented to furnish time histories of control surface positions, it is then theoretically possible by means of digital filtering procedures, to correct the response data for the effects of control surface deflections induced by the pilot or by automatic control systems. The filters would be derived from the analytical model as indicated in the figure.

5.3 APPLICATIONS TO AIRCRAFT DESIGN PROCEDURES

Cumulative fatigue damage as calculated by Miner's theory is proportional to zero crossing rate, but is usually much more sensitive to rms load amplitude, so that even a small change in the latter quantity can have a significant effect on fatigue life. It is therefore recommended that load data furnished by 1-D and 3-D gust response analysis be applied to obtain a comparison of the effects of the two gust response models on calculated fatigue damage. Comparisons with fatigue damage estimates derived from fatigue testing and aircraft utilization would also be conducted. The airplane treated in Paragraphs 5.1 and 5.2 can be used in the verification.

Since the 1-D turbulence field retains full spatial coherence, the magnitude gust response effects in the 3-D case is ultimately dependent upon the reduction in coherence between input gust forces. Gust forces acting upon a given panel depend on the gust normalwash impinging upon neighboring panels as well as upon the given panel itself. Although modified strip theory accounts for the induction effects of neighboring panels, it attributes the total gust force on each panel to the normalwash impinging upon that panel alone. Then gust force coherence becomes identical to gust normalwash coherence, which is determined solely by the turbulence field as described in Paragraph 2.3.

Therefore, only by the application of aerodynamic methods which treat induction effects explicitly can the influence of aerodynamics on gust force coherence be accounted for. This is feasible for routine gust design calculations in the supersonic case (Mach

box methods, for example.) However, in the subsonic case, the computational effort required has often discouraged routine use of methods such as the doublet lattice. A new subsonic kernel function formulation described in Appendix B has been developed to remedy this deficiency by allowing much of the computational effort currently involved in the application of doublet lattice methods to be replaced by simple tabular interpolation. It is therefore recommended that computational procedures which fully exploit the new method be made available, including tables of the necessary aerodynamic data. Analytical data on the spatial coherence distribution of gust force for simple configurations should also be provided in the form of plots or tables. This would allow aerodynamic effects to be considered in investigating the spatial coherence distribution of gust force for 3-D gust response calculations.

5.4 ADVANCED DEVELOPMENT

The three-dimensional gust response analysis developed in Section II is capable of accounting for all three gust components simultaneously, as explained in Paragraph 2.7. To exploit this capability, further development is recommended to provide an improved aerodynamic representation for longitudinal gust response. Current gust response models usually ignore the longitudinal component, as explained in Paragraph 4.4.

Since pilot-induced control surface deflections which occur during dynamic response test flights in turbulence cannot be accurately treated by linear response methods, no attempt is made

Contrails

to incorporate a description of the resulting structural responses into the analytical model used in flight test comparisons. Since these responses are not insignificant, it is recommended that high speed digital filtering techniques be developed to correct the measured responses for control effects. Fast Fourier transform methods could be employed to generate filters corresponding to the frequency response functions which relate these structural responses to the control surface deflections. The filters could be applied to the measured control surface deflections to obtain time histories of the resulting responses. These could then be deducted from the corresponding measured responses to correct for control inputs. The process is illustrated in Figure 18.

Current gust criteria and load computation methods could be extended to include phenomena which depart from Taylor's hypothesis and the assumption of homogeneity, which are introduced in Appendix A. Nonhomogeneity is exemplified by the "patchy" character of medium and high altitude turbulence and by low altitude turbulence induced by ground obstructions. Such diverse phenomena as enhanced small sample variability, non-Gaussian statistical effects and flattened gust power spectra may be attributed to nonhomogeneity. Similarly, the "frozen" turbulence assumption represented by equation A-4 may be invalid at the very low airspeeds to which helicopters or VSTOL aircraft are subject.

REFERENCES

1. Liepmann, H. W., "Extension of the Statistical Approach to Buffeting and Gust Response of Wings of Finite Span," Journal of the Aeronautical Sciences, Vol. 22, No. 3, March 1955, pp. 197-200
2. Ribner, H. S., "Spectral Theory of Buffeting and Gust Response: Unification and Extension," Journal of the Aeronautical Sciences, Vol. 23, No. 12, Dec. 1956, pp. 1075-1077, 1118
3. Etkin, B., "A Theory of the Response of Airplanes to Random Atmospheric Turbulence," Journal of the Aerospace Sciences, Vol. 26, No. 7, July 1959, pp. 409-420
4. Beer, F. P., and Ravera, R. J., "Effect of Spacewise Variations in a Random Load Field on the Response of Linear System," AIAA Journal, Vol. 4, 1966, pp. 1651-1654
5. Diederich, F. W., "The Dynamic Response of a Large Airplane to Continuous Random Atmospheric Disturbances," Journal of the Aeronautical Sciences, Vol. 23, No. 10, Oct. 1956, pp. 917-930
6. Houbolt, J. C., "Design Manual for Vertical Gusts Based on Power Spectral Techniques", TR-70-106, December 1970, AFFDL
7. Coupry, G., "Effect of Spanwise Variation of Gust Velocity on Airplane Response to Turbulence," Journal of Aircraft, Vol. 9, No. 8, Aug. 1972, pp. 569-574

REFERENCES (Continued)

8. Fuller, J. R., "A Procedure for Evaluating the Spacewise Variations of Continuous Turbulence on Airplane Responses," Journal of Aircraft, Vol. 5, No. 1, Jan.-Feb. 1968, pp. 49-50
9. Eichenbaum, F. D., "A General Theory of Aircraft Response to Three-Dimensional Turbulence," Journal of Aircraft, Vol. 8, No. 5, May 1971, pp. 353-360
10. Ingram, C. T. and Eichenbaum, F. D., "A Comparison of C-141A Flight Test Measured and Theoretical Vertical Gust Responses," Journal of Aircraft, Vol. 6, No. 6, Nov.-Dec. 1969, pp. 532-536
11. Jones, J. W., Mielke, R. H., Jones, G. W., et al, "Low Altitude Atmospheric Turbulence LO-LOCAT Phase III", TR-70-10, Vols. I and II, November 1970, AFFDL
12. Landahl, M. T., "Kernel Function for Nonplanar Oscillating Surfaces in a Subsonic Flow", AIAA Journal, Vol. 5, No. 5, May 1967, pp. 1045-1046
13. Watkins, C. E., Woolston, D. S., and Cunningham, H. J., "A Systematic Kernel Function Procedure for Determining Aerodynamic Forces on Oscillating or Steady Finite Wings at Subsonic Speeds", TR R-48, 1959, NASA
14. Laschka, B., "Zur Theorie der harmonisch schwingender tragenden Fläche Bei Unterschallströmung", Zeitschrift für Flugwissenschaften, Vol. 1, No. 7, July 1963, pp. 265-292

REFERENCES (Continued)

15. Hastings, C., Jr., Approximations for Digital Computers, Princeton University Press, 1955
16. Filon, L. N. G., Proceedings of the Royal Society of Edinburgh, Vol. 49, 1928-1929, pp. 38-47
17. Rodden, W. P., Giesing, J. P., and Kalman, T. P., "Refinement of the Nonplanar Aspects of the Subsonic Doublet-Lattice Lifting Surface Method", Journal of Aircraft, Vol. 9, No. 1, January 1972

APPENDIX A

A DUAL GUST RESPONSE FORMULATION

The dynamic response of an aircraft traversing a three-dimensional field of atmospheric turbulence may be described by either of two equivalent mathematical forms, which differ according to whether the vector frequency response function which describes the aircraft, and the tensor function which describes the turbulence field, are expressed in the space domain or in the wave domain. Conversion of a function from one domain to the other is accomplished by applying a three-dimensional Fourier transformation.

A.1 SPACE DOMAIN

The space domain version of the three-dimensional gust response problem may be derived by substituting the convolution expression for the response,

$$X(t) = \int \mathbf{h}(\mathbf{r}, \tau) \cdot \mathbf{u}(\mathbf{r}, t-\tau) d\mathbf{r} d\tau \quad (\text{A-1})$$

into the definition of the response autocorrelation function to obtain

$$\begin{aligned} C(\tau) &= \left\langle \int \mathbf{h}(\mathbf{r}, \alpha) \cdot \mathbf{u}(\mathbf{r}, t-\alpha) d\mathbf{r} d\alpha \int \mathbf{h}(\mathbf{s}, \beta) \cdot \mathbf{u}(\mathbf{s}, t+\tau-\beta) d\mathbf{s} d\beta \right\rangle \\ &= \int \mathbf{h}(\mathbf{r}, \alpha) \cdot \left\langle \mathbf{u}(\mathbf{r}, t-\alpha) \mathbf{u}(\mathbf{s}, t+\tau-\beta) \right\rangle \cdot \mathbf{h}(\mathbf{s}, \beta) d\mathbf{r} d\mathbf{s} d\alpha d\beta \\ &= \int \mathbf{h}(\mathbf{r}, \alpha) \cdot \mathbf{Q}(\mathbf{s}-\mathbf{r}, \tau+\alpha-\beta) \cdot \mathbf{h}(\mathbf{s}, \beta) d\mathbf{r} d\mathbf{s} d\alpha d\beta \end{aligned} \quad (\text{A-2})$$

where the brackets, $\langle \rangle$, denote the time average.

Contrails

The assumption that the gust velocity correlation tensor is a function only of the space-time separation between the points at which the velocity is measured implies that the turbulence field is homogeneous and stationary; i.e., the statistical properties are independent of position and time.

The gust velocity correlation tensor in the moving reference frame may be replaced by its equivalent in the fixed reference frame by recognizing that the input point \mathbf{s} has moved an additional distance $(\tau+\alpha-\beta)\mathbf{U}$ relative to \mathbf{r} when both points are measured in the fixed reference frame. Thus,

$$\mathbf{Q}(\mathbf{s}-\mathbf{r}, \tau+\alpha-\beta) = \mathbf{R}(\mathbf{s}-\mathbf{r}+(\tau+\alpha-\beta)\mathbf{U}, \tau+\alpha-\beta) \quad (\text{A-3})$$

Furthermore, by assuming that the input turbulence field is "frozen" according to Taylor's hypothesis, we may set

$$\mathbf{R}(\mathbf{s}-\mathbf{r}+(\tau+\alpha-\beta)\mathbf{U}, \tau+\alpha-\beta) = \mathbf{R}(\mathbf{s}-\mathbf{r}+(\tau+\alpha-\beta)\mathbf{U}, 0) \quad (\text{A-4})$$

Substituting these results and equation (A-2) into the definition for the response power spectrum, replacing $\tau+\alpha-\beta$ by a single variable and invoking the appropriate definitions then yields

$$\begin{aligned} \phi(f) &= 2 \int \mathbf{h}(\mathbf{r}, \alpha) \cdot \mathbf{R}(\mathbf{s}-\mathbf{r}+(\tau+\alpha-\beta)\mathbf{U}, 0) \cdot \mathbf{h}(\mathbf{s}, \beta) e^{-2\pi i f \tau} d\mathbf{r} d\mathbf{s} d\alpha d\beta d\tau \\ &= 2 \int \mathbf{h}(\mathbf{r}, \alpha) \cdot \mathbf{R}(\mathbf{s}-\mathbf{r}+\mathbf{U}\tau, 0) \cdot \mathbf{h}(\mathbf{s}, \beta) e^{-2\pi i f (\tau-\alpha+\beta)} d\mathbf{r} d\mathbf{s} d\alpha d\beta d\tau \\ &= \int \left\{ \int \mathbf{h}(\mathbf{r}, \alpha) e^{2\pi i f \alpha} d\alpha \right\} \cdot \left\{ 2 \int \mathbf{R}(\mathbf{s}-\mathbf{r}+\mathbf{U}\tau, 0) e^{-2\pi i f \tau} d\tau \right\} \cdot \\ &\quad \left\{ \int \mathbf{h}(\mathbf{s}, \beta) e^{-2\pi i f \beta} d\beta \right\} d\mathbf{r} d\mathbf{s} \\ &= \int \mathbf{H}^*(\mathbf{r}, f) \cdot \Phi(\mathbf{s}-\mathbf{r}, f) \cdot \mathbf{H}(\mathbf{s}, f) d\mathbf{r} d\mathbf{s} \quad (\text{A-5}) \end{aligned}$$

Equation (A-5) represents the space domain formulation of the three-dimensional gust response problem. Since the frequency response functions are normalized to surface area and vanish off the aerodynamic surfaces, the double volume integral of equation (A-5) effectively reduces to a finite double surface integral. Furthermore, analytical expressions for the gust velocity cross spectrum tensor are derivable from any of the common isotropic turbulence models such as the Dryden or von Karman. Notice that these tensors in general are of second rank and therefore have nine components, one for each ordered pair of Cartesian coordinates.

A.2 WAVE DOMAIN

The space domain formulation of the gust response problem may be converted into the wave domain version, but it is first necessary to derive an alternative expression for the velocity cross spectrum tensor by transforming it to the wave domain and back, and employing the Dirac delta function. The forward transformation yields

$$\int \Phi(\mathbf{r}, f) e^{-i\boldsymbol{\Omega} \cdot \mathbf{r}} d\mathbf{r} = 2 \int \mathbf{R}(\mathbf{r} + \mathbf{U}\tau, 0) e^{-i(\boldsymbol{\Omega} \cdot \mathbf{r} + 2\pi f\tau)} d\mathbf{r} d\tau \quad (\text{A-6})$$

By adding and subtracting $\boldsymbol{\Omega} \cdot \mathbf{U}\tau$, the bracketted expression in the exponent on the right hand side can be rewritten

$$\boldsymbol{\Omega} \cdot \mathbf{r} + 2\pi f\tau = \boldsymbol{\Omega} \cdot (\mathbf{r} + \mathbf{U}\tau) + (2\pi f - \boldsymbol{\Omega} \cdot \mathbf{U})\tau \quad (\text{A-7})$$

Substituting this result into equation (A-6) and letting $\mathbf{q} = \mathbf{r} + \mathbf{U}\tau$

then yields

$$\begin{aligned} \int \Phi(\mathbf{r}, f) e^{-i\boldsymbol{\Omega} \cdot \mathbf{r}} d\mathbf{r} &= 2 \int e^{-i(2\pi f - \boldsymbol{\Omega} \cdot \mathbf{U})\tau} d\tau \int \mathbf{R}(\mathbf{q}, 0) e^{-i\boldsymbol{\Omega} \cdot \mathbf{q}} d\mathbf{q} \\ &= 32\pi^4 \delta(2\pi f - \boldsymbol{\Omega} \cdot \mathbf{U}) \mathbf{S}(\boldsymbol{\Omega}) \end{aligned} \quad (\text{A-8})$$

If the Fourier transformation back to the space domain is applied to both sides of equation (A-8), we obtain

$$\begin{aligned} (1/2\pi)^3 \int \Phi(\mathbf{r}, f) e^{-i\boldsymbol{\Omega} \cdot (\mathbf{r} - \mathbf{s})} d\boldsymbol{\Omega} d\mathbf{r} &= (1/2\pi)^3 \int \Phi(\mathbf{r}, f) 8\pi^3 \delta(\mathbf{r} - \mathbf{s}) d\mathbf{r} \\ &= 32\pi^4 (1/2\pi)^3 \int \delta(2\pi f - \boldsymbol{\Omega} \cdot \mathbf{U}) \mathbf{S}(\boldsymbol{\Omega}) e^{i\boldsymbol{\Omega} \cdot \mathbf{s}} d\boldsymbol{\Omega} \\ \Phi(\mathbf{s}, f) &= 4\pi \int \delta(2\pi f - \boldsymbol{\Omega} \cdot \mathbf{U}) \mathbf{S}(\boldsymbol{\Omega}) e^{i\boldsymbol{\Omega} \cdot \mathbf{s}} d\boldsymbol{\Omega} \end{aligned} \quad (\text{A-9})$$

The wave domain formulation can now be derived by substituting equation (A-9) into (A-5) and applying the definition of the frequency response function in the wave domain. Thus,

$$\begin{aligned} \phi(f) &= \int \mathbf{H}^*(\mathbf{r}, f) \cdot \left\{ 4\pi \int \delta(2\pi f - \boldsymbol{\Omega} \cdot \mathbf{U}) \mathbf{S}(\boldsymbol{\Omega}) e^{i\boldsymbol{\Omega} \cdot (\mathbf{s} - \mathbf{r})} d\boldsymbol{\Omega} \right\} \cdot \mathbf{H}(\mathbf{s}, f) d\mathbf{r} d\mathbf{s} \\ &= 4\pi \int \delta(2\pi f - \boldsymbol{\Omega} \cdot \mathbf{U}) \left\{ \int \mathbf{H}^*(\mathbf{r}, f) e^{-i\boldsymbol{\Omega} \cdot \mathbf{r}} d\mathbf{r} \right\} \cdot \mathbf{S}(\boldsymbol{\Omega}) \cdot \left\{ \int \mathbf{H}(\mathbf{s}, f) e^{i\boldsymbol{\Omega} \cdot \mathbf{s}} d\mathbf{s} \right\} d\boldsymbol{\Omega} \\ &= 4\pi \int \delta(2\pi f + \boldsymbol{\Omega}_1 \cdot \mathbf{U}) \mathbf{K}^*(\boldsymbol{\Omega}, f) \cdot \mathbf{S}(\boldsymbol{\Omega}) \cdot \mathbf{K}(\boldsymbol{\Omega}, f) d\boldsymbol{\Omega} \end{aligned} \quad (\text{A-10})$$

Equation (A-10) represents the wave domain formulation of the three-dimensional gust response problem. The effect of the delta function in the integrand is to extract those spatial waves which contribute to the frequency f . Analytical expressions for the tensor components of $\mathbf{S}(\boldsymbol{\Omega})$ are derivable from the common spectral models for isotropic turbulence. However, except in certain rudimentary cases, it is generally impractical to compute $\mathbf{K}(\boldsymbol{\Omega}, f)$ directly from its definition. A procedure has therefore been developed which may be

derived by expanding the definition of $\mathbf{K}(\Omega, f)$ in a Maclaurin series,

$$\begin{aligned} \mathbf{K}(\Omega, f) &= \sum_{n=0}^{\infty} (1/n!) (\Omega \cdot \nabla')^n \mathbf{K}(\Omega', f) \Big|_{\Omega'=\mathbf{0}} \\ &= \sum_{n=0}^{\infty} (1/n!) \int \mathbf{H}(\mathbf{r}, f) (\Omega \cdot \nabla')^n e^{i\Omega' \cdot \mathbf{r}} d\mathbf{r} \Big|_{\Omega'=\mathbf{0}} \\ &= \sum_{n=0}^{\infty} (1/n!) \int \mathbf{H}(\mathbf{r}, f) (i\Omega \cdot \mathbf{r})^n d\mathbf{r} \end{aligned} \quad (\text{A-11})$$

where $\nabla' = \mathbf{i} \partial / \partial \Omega_1' + \mathbf{j} \partial / \partial \Omega_2' + \mathbf{k} \partial / \partial \Omega_3'$ is the gradient operator in wave number space, and $\mathbf{i}, \mathbf{j}, \mathbf{k}$ are unit vectors parallel to the corresponding wave number axes. Substituting this result into equation (A-10), integrating over Ω_1 , and grouping terms in like powers of Ω_2 and Ω_3 , we obtain

$$\phi(f) = \sum_{n,m,l=0}^{\infty} \sum_{k,j,i=0}^{n,m,l} \mathbf{H}^*(f)_{ijk} \cdot \mathbf{S}(f)_{mn} \cdot \mathbf{H}(f)_{l-i,m-j,n-k} \quad (\text{A-12})$$

where $\mathbf{H}(f)_{ijk} = [(\sqrt{-1})^{i+j+k} (-2\pi f/U)^i / i!j!k!] \int \mathbf{H}(\mathbf{r}, f) r_1^i r_2^j r_3^k d\mathbf{r}$

and $\mathbf{S}(f)_{mn} = \int \mathbf{S}(-2\pi f/U, \Omega_2, \Omega_3) \Omega_2^m \Omega_3^n d\Omega_2 d\Omega_3$

are moments of the vector frequency response function in the space domain, and the gust velocity power spectrum tensor in the wave domain, respectively. The summation order is from right to left.

Equation (A-12) is eminently suitable for machine computation because its generalized form facilitates inclusion of higher order terms which are significant at higher response frequencies. When

$\mathbf{S}(\Omega)$ is derived from the Dryden or von Karman spectral models, a wave number cutoff must be imposed to prevent divergence of its higher moments. The influence of this cutoff on the convergence properties of the expansion warrants further investigation.

APPENDIX B

AN IMPROVED KERNEL FUNCTION FORMULATION FOR UNSTEADY SUBSONIC FLOW

The application of doublet lattice methods to nonplanar surfaces in unsteady, subsonic flow has often been discouraged by the elaborate approximation procedures required to evaluate the kernel function. A new formulation is presented which allows these lengthy calculations to be replaced by simple, accurate tabular interpolations, thereby yielding a significant reduction of computational effort in typical applications.

Let x_0 , y_0 , and z_0 denote the Cartesian coordinates of a normalwash point relative to an oscillating pressure dipole of strength $pe^{i\omega t}$, and let γ_r and γ_s represent the dihedral angles of the surfaces at the respective receiving and sending points. Then the ratio of the normalwash w/U to the lift exerted by the pressure dipole is given by the kernel function*

$$K = e^{-i\omega x_0/U} (K_1 T_1 - K_2 T_2) / 8\pi q r_1^2$$

where U is the airspeed, q is the dynamic pressure,

$r_1 = (y_0^2 + z_0^2)^{1/2}$, and the relative orientation between surfaces is accounted for by

$$T_1 = \cos(\gamma_r - \gamma_s)$$

and $T_2 = (z_0 \cos \gamma_r - y_0 \sin \gamma_r)(z_0 \cos \gamma_s - y_0 \sin \gamma_s) / r_1^2$

*For notational brevity in the development which follows, the sign of K_2 is reversed relative to convention.

Contrails

The expressions for K_1 and K_2 given by Landahl (Reference 12) contain the integrals

$$I_\nu(k_1, u_1) = \int_{u_1}^{\infty} \frac{e^{-ik_1 u}}{(1+u^2)^{\nu+1/2}} du \quad \nu = 1, 2$$

where $k_1 = \omega r_1 / U$, $u_1 = (MR - x_0) / \beta^2 r_1$, $R = (x_0^2 + \beta^2 r_1^2)^{1/2}$, $\beta = (1 - M^2)^{1/2}$ and $M =$ Mach number. For convenience, define

$$K_\nu' = e^{ik_1 u_1} K_\nu \quad \nu = 1, 2$$

Then the kernel function may be rewritten

$$K = e^{-i\omega M(R - Mx_0) / \beta^2 U} (K_1' T_1 - K_2' T_2) / 8\pi q r_1^2$$

I_1 and I_2 cannot be evaluated in closed form unless $k_1 = 0$ or $u_1 = 0$. Moreover, each integral generates a family of spirals having u_1 as parameter and converging toward the origin of the complex plane as k_1 increases. (See Figure 19.) Because of this complicated behavior, it has been more practical to compute the integrals as needed by lengthy approximation procedures (References 13 and 14), than to furnish them directly by tabular interpolation. However, by defining a new function

$$F_\nu(k_1, u_1) = (2\nu - 1) e^{ik_1 u_1} I_\nu(k_1, u_1) \quad \nu = 1, 2$$

the spirals are effectively unwound and confined to a single quadrant. It is actually most convenient to tabulate F_ν in its normalized form

$$\bar{F}_\nu(k_1, u_1) = F_\nu(k_1, u_1) / F_\nu(0, u_1) \quad \nu = 1, 2$$

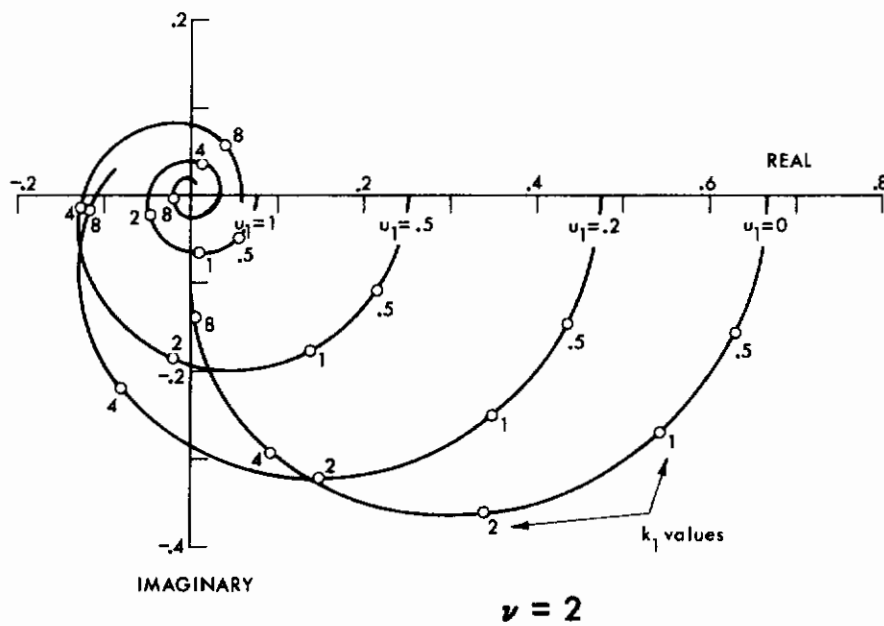
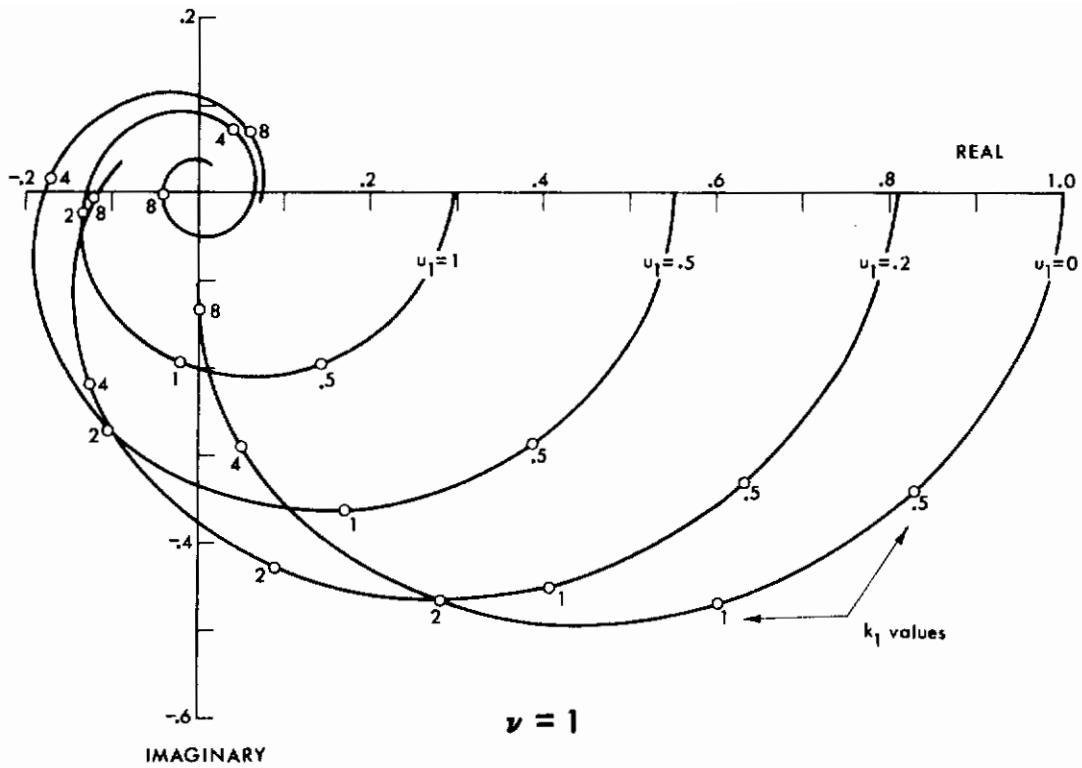


Figure 19. Behavior of the Integrals, $I_\nu(k_1, u_1)$, Occurring in the Conventional Version of the Nonplanar Acceleration Potential Kernel for Oscillating Subsonic Flow

Contrails

where $F_1(0, u_1) = 1 - u_1/(1+u_1^2)^{1/2}$

and $F_2(0, u_1) = 2F_1(0, u_1) - u_1/(1+u_1^2)^{3/2}$

For large values of u_1 , \bar{F}_ν may be replaced by its asymptotic form \tilde{F}_ν . Thus,

$$\bar{F}_\nu(k_1, u_1) \approx \tilde{F}_\nu(k_1 u_1) \quad \text{for } u_1^2 \gg 1 \quad \nu = 1, 2$$

where $\tilde{F}_\nu(k_1 u_1) = 2^\nu u_1^{2\nu} e^{ik_1 u_1} \int_{u_1}^{\infty} u^{-2\nu-1} e^{-ik_1 u} du$

This expression may be integrated by parts to yield

$$\tilde{F}_1(k_1 u_1) = 1 - (k_1 u_1)^2 g(k_1 u_1) + i \left[-k_1 u_1 + (k_1 u_1)^2 f(k_1 u_1) \right]$$

$$\begin{aligned} \tilde{F}_2(k_1 u_1) = & 1 - \left[(k_1 u_1)^2 + (k_1 u_1)^4 g(k_1 u_1) \right] / 6 \\ & + i \left[-2k_1 u_1 + (k_1 u_1)^3 - (k_1 u_1)^4 f(k_1 u_1) \right] / 6 \end{aligned}$$

where $f(k_1 u_1) = \int_0^\infty \frac{\sin u}{u + k_1 u_1} du$ and $g(k_1 u_1) = \int_0^\infty \frac{\cos u}{u + k_1 u_1} du$ are

auxiliary functions or which accurate approximations are available (Reference 15). For moderate values of u_1 , \bar{F}_ν may be computed by dividing the range of integration of $I_\nu(k_1, u_1)$ into two parts, choosing the upper limit of the first integral large enough so that the second integral may be written approximately in terms of \tilde{F}_ν .

Then

$$\bar{F}_\nu(k_1, u_1) \approx \frac{2^\nu - 1}{F_\nu(0, u_1)} e^{ik_1 u_1} \left[\int_{u_1}^{\tilde{u}} \frac{e^{-ik_1 u}}{(1+u^2)^{\nu+1/2}} du + \frac{\tilde{F}_\nu(k_1 \tilde{u})}{2^\nu \tilde{u}^{2\nu}} e^{-ik_1 \tilde{u}} \right]$$

for $\tilde{u}^2 \gg 1 \quad \nu = 1, 2$

Contrails

A numerical evaluation of the first integral may be efficiently accomplished by Filon's method (Reference 16), in which the integration interval is divided into an even number of equal increments. Since the exponential in the integral varies rapidly with u when k_1 is large, it is treated exactly, whereas the remainder of the integrand, which varies smoothly, is fitted with a parabola over each double increment in u . Tables are easily constructed by this method to provide interpolated \bar{F}_ν values of greater accuracy than corresponding values of I_ν computed by conventional approximation methods. The tables need not extend to $u_1 < 0$, since

$$F_\nu(k_1, -u_1)' = 2 e^{-ik_1 u_1} \text{Re} [F_\nu(k_1, 0)] - F_\nu^*(k_1, u_1)$$

where $\nu = 1, 2$ and the asterisk denotes the complex conjugate.

\bar{F}_ν is conveniently tabulated vs k_1 and u_1 if u_1 is small. However, the expressions for \tilde{F}_ν suggest that for larger values of u_1 , it would be more appropriate to replace the parameter k_1 by $k_1 u_1$. In keeping with this arrangement, curves of \bar{F}_ν are plotted in Figure 20 for constant u_1 , and also for constant k_1 over the range $0 \leq u_1 \leq 1$, and for constant $k_1 u_1$ over the range $1 \leq u_1 \leq \infty$. Physical considerations will inevitably dictate an upper limit for k_1 when u_1 is small and for $k_1 u_1$ when u_1 is large, thereby providing further justification for the split table.

Under the new formulation, the expressions for K_1' and K_2' may be written

$$K_1'(M, k_1, u_1) = F_1(k_1, u_1) + G_1(M, u_1)$$

$$K_2'(M, k_1, u_1) = F_2(k_1, u_1) + ik_1 \theta \delta^2 + G_2(M, u_1)$$

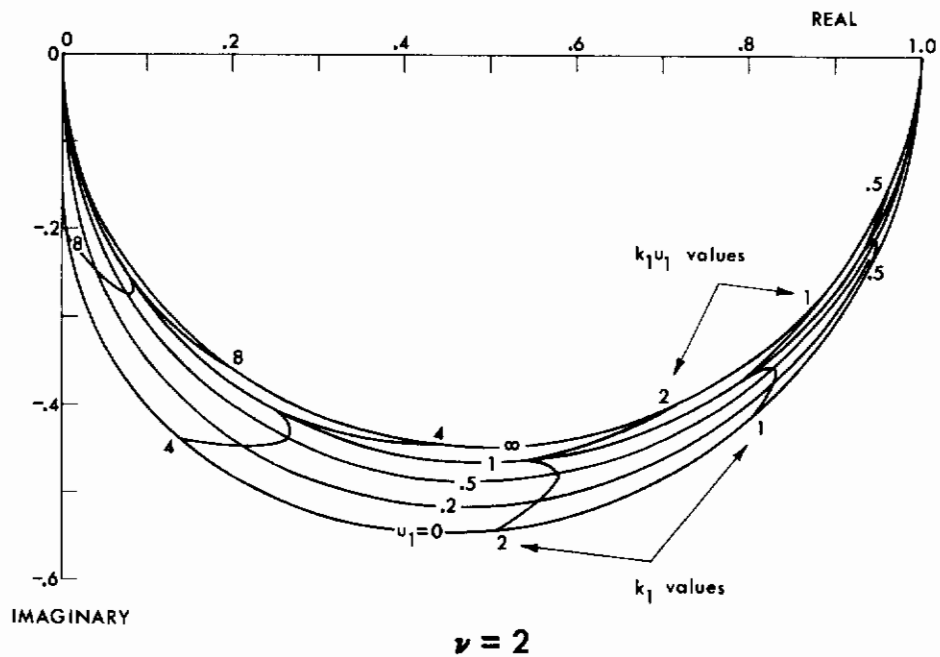
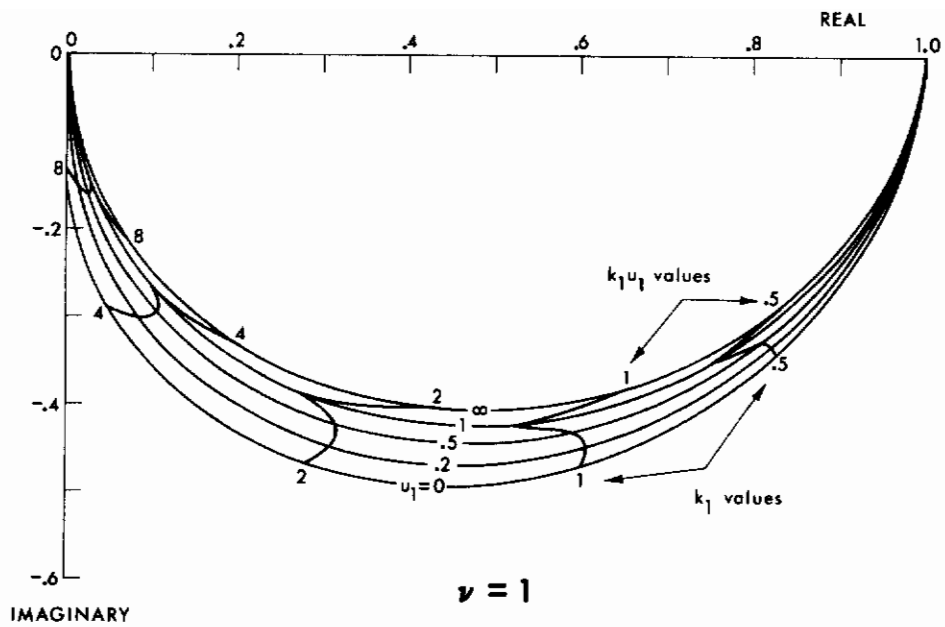


Figure 20. Behavior of the Integrals, $\bar{F}_\nu(k_1, u_1)$, Occurring in the New Formulation of the Nonplanar Acceleration Potential Kernel for Oscillating Subsonic Flow

Contrails

where $\theta(u_1) = (1+u_1^2)^{-1/2}$ and $\delta(M, u_1) = M(Mu_1 + 1/\theta) / (1+\beta^2 u_1^2) = Mr_1/R$

are introduced as computational parameters. Then

$$G_1(M, u_1) = \theta \delta$$

$$G_2(M, u_1) = \theta \delta \left[\theta^2 (u_1 \delta + 2) + \delta^2 (\beta/M)^2 \right]$$

Quantities such as G_1 and G_2 which are independent of angular frequency ω need be computed only once for any given geometrical configuration. Furthermore, when the flow regime is restricted to the incompressible or steady state cases, K_1' and K_2' reduce to

$$K_\nu'(M, 0, u_1) = F_\nu(0, u_1) + G_\nu(M, u_1) \quad \text{STEADY FLOW}$$

$$K_\nu'(0, k_1, u_0) = F_\nu(k_1, u_0) \quad \text{INCOMPRESSIBLE FLOW}$$

$$K_\nu'(0, 0, u_0) = F_\nu(0, u_0) \quad \text{STEADY, INCOMPRESSIBLE FLOW}$$

where $\nu = 1, 2$ and $u_0 = -x_0/r_1$

The only singularity in the kernel occurs when $r_1 \rightarrow 0$ and the normalwash point lies in the wake of the pressure dipole. In that case, $K_\nu \rightarrow F_\nu \rightarrow 2\nu$. Procedures for treating the singularity have been described elsewhere (Reference 17), and are compatible with the formulation presented here.

Contrails

Unclassified

Security Classification

DOCUMENT CONTROL DATA - R & D		
<i>(Security classification of title, body of abstract and indexing annotation must be entered when the overall report is classified)</i>		
1. ORIGINATING ACTIVITY (Corporate author)		2a. REPORT SECURITY CLASSIFICATION
Lockheed-Georgia Company		Unclassified
		2b. GROUP
3. REPORT TITLE		
RESPONSE OF AIRCRAFT TO THREE-DIMENSIONAL RANDOM TURBULENCE		
4. DESCRIPTIVE NOTES (Type of report and inclusive dates)		
5. AUTHOR(S) (First name, middle initial, last name)		
Frederick D. Eichenbaum		
6. REPORT DATE	7a. TOTAL NO. OF PAGES	7b. NO. OF REFS
October 1972	83	17
8a. CONTRACT OR GRANT NO.	9a. ORIGINATOR'S REPORT NUMBER(S)	
F33615-71-C-1878		
b. PROJECT NO. 1367		
c. TASK NO. 136702	9b. OTHER REPORT NO(S) (Any other numbers that may be assigned this report)	
d.	AFFDL-TR-72-28	
10. DISTRIBUTION STATEMENT		
Approved for public release; distribution unlimited.		
11. SUPPLEMENTARY NOTES	12. SPONSORING MILITARY ACTIVITY	
	Air Force Flight Dynamics Laboratory FBE Wright-Patterson AFB, Ohio 45433	
13. ABSTRACT		
<p>Conceptually possible procedures for designing aircraft for the combined effects of vertical, lateral, and longitudinal turbulence by the application of power spectral techniques are developed and outlined. The present state-of-the-art of this technical area is established and evaluated by reviewing and extending current methods used or proposed for predicting the response of aircraft due to combined effects of the three components of atmospheric turbulence. Requirements for solving the problem are identified and recommendations are made with respect to major problem areas such as: description of the turbulence environment, determination of the frequency response function of the structure, and methods of combining the effects of vertical, lateral and longitudinal turbulence components to theoretically predict aircraft response. Finally, an outline of the specific research needed is given, and a program is presented for accomplishing the research and development required to solve the problem.</p>		

DD FORM 1 NOV 65 1473

Unclassified

Security Classification

Unclassified

Security Classification

14. KEY WORDS	LINK A		LINK B		LINK C	
	ROLE	WT	ROLE	WT	ROLE	WT
Three-Dimensional Turbulence Gust Loads Power Spectra Transfer Functions Aircraft Structures Dynamic Response Analysis						

Unclassified

Security Classification